

Comprehensive Analysis of Geometric Hole Designs and Configurations in Film Cooling for Gas Turbine Engines: A Critical Review

Muhammad Fitri Mohd Zulkeple ¹, Abd Rahim Abu Talib ^{1,2*}, Mohammad Yazdi Harmin ¹, Syamimi Saadon ¹, Muhammad Hanafi Azami ³, Talal Yusaf ⁴

¹*Aerodynamics, Heat Transfer & Propulsion (AHTP) Research Group, Department of Aerospace Engineering, Faculty of Engineering, Universiti Putra Malaysia, 43400 Serdang, Selangor, Malaysia*

²*Aerospace Malaysia Research Centre, Faculty of Engineering, Universiti Putra Malaysia, 43400 Serdang, Selangor, Malaysia*

³*Kulliyah of Engineering, International Islamic University Malaysia, P.O. Box 10, 50728 Kuala Lumpur, Malaysia*

⁴*School of Engineering and Technology, Central Queensland University, Australia*

ABSTRACT

This paper provides a comprehensive review of the geometric design and configuration of film cooling holes. It highlights a critical concern in film cooling, which is the interaction between the main airflow and the cooling jet emerging from the holes. This interaction significantly influences various factors associated with hole design, including the length-to-diameter ratio (L/D), the exit-to-inlet cross-sectional area ratio (AR), the pitch-to-diameter ratio (P/D), and the compound angle of the hole. Furthermore, the paper discusses the introduction of flow disturbances, such as vortex generators, upstream of the cooling holes, as well as the construction of trenches around these holes. These modifications aim to alter the behaviour of the boundary-layer flow and its interaction with the film-cooling jet. The paper offers a comprehensive examination of these aspects, shedding light on the complex relationship between geometric design, flow modification, and film cooling effectiveness. Over time, hole design has evolved from cylindrical shapes to more complex designs, which improved cooling. Longer holes ($L/D > 3$) perform better in film cooling than short holes ($L/D \leq 3$) due to fully developed coolant flow. The aspect ratio and pitch affect coolant distribution, and compound angled holes improve lateral coverage. According to the literature covered in this study, film cooling has progressed in several design characteristics. However, the adjustments made are not an instant fix for this method defects. Future research should develop unique approaches and optimizations to solve film cooling's problems and complexities.

Keywords: cooling, Gas turbine engine, Hole design, Comprehensive review.

I. INTRODUCTION

Aircraft design and performance have been consistently improving over the recent years. Recent advancements in aircraft aerodynamics [1], gas turbine efficiency [2,3], advanced control systems, and the

development of new sustainable materials [4,5] are the focal points of interest.

The combustion chamber, or burner, plays a pivotal role in a gas turbine engine, where it converts chemical energy into thermal energy to extract work. Consequently, the combustion chamber wall or liner is exposed to heat transfer through all three modes: conduction, convection,

and radiation, as depicted in Figure 1. The liner's side is heated by the radiation from the flame and the convection of the hot combustion gases. This, in turn, leads to axial and radial conduction across the liner [6].

As the temperature within the chamber increases to mitigate emissions from the engine, the heat load on the liner intensifies. This poses a significant challenge regarding the liner's ability to function effectively under such extreme conditions. Over the past few decades, extensive research and development efforts have been undertaken to safeguard the liner. These efforts involve utilizing bleed air from the compressor and applying coatings with low thermal conductivity to the liner's side. These cooling techniques have evolved and undergone various improvements to enhance their effectiveness in cooling the liner. In some cases, combined cooling techniques have been implemented to optimize the liner's performance.

Various cooling techniques have been employed to ensure the long-term durability of the combustion chamber liner. These innovations range from basic film cooling to transpiration cooling, which utilizes porous materials to dissipate heat from the surface. Numerous experimental and numerical studies have showcased their effectiveness in addressing advanced cooling challenges [7,8].

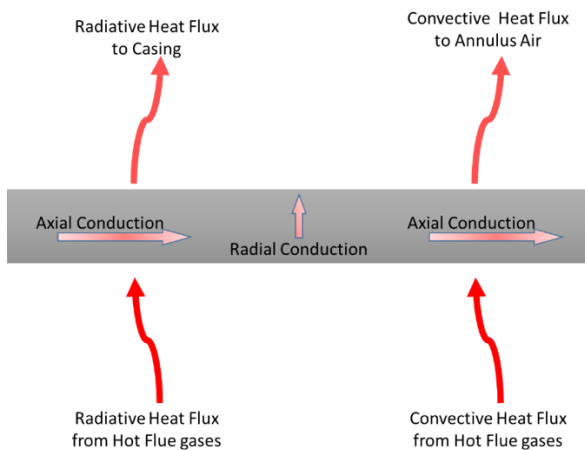


Figure 1 Heat load on the combustion liner [6]

The most common cooling employed is film cooling where compressor bleed air is directed through holes to create a protective air film on the liner's surface, shielding it from the high-temperature gases. However, this method has a drawback: it doesn't fully maximize the cooling potential despite consuming a significant portion of the incoming airflow [9].

On the other hand, transpiration cooling, also known as porous liner cooling, combines convection within a porous medium with external film cooling, enhancing thermal performance and cooling efficiency compared to other methods [10]. Nonetheless, it is susceptible to clogging due to combustion residue, stemming from its structural design. To overcome this limitation, effusion cooling was introduced, resembling transpiration cooling but with minor performance trade-offs [11]. Effusion cooling involves multiple arrays of small holes that act as

both a film and transpiration cooling system, reducing coolant usage while preventing clogging.

Another popular technique among researchers is impingement cooling, comprising a series of heat sink plates (the liner) struck by coolant directed from the compressor through various holes. According to Chi et al., [12], this method offers high heat transfer intensity and flow resistance, piquing the interest of heat transfer researchers. In some cases, impingement cooling is combined with effusion techniques to optimize coolant effectiveness on the liner's surface.

The primary objective of this paper is to comprehensively examine and assess various innovative cooling techniques employed in gas turbine engine combustion chambers. These techniques play a critical role in preserving the long-term sustainability and efficiency of combustion chamber liners, which are subjected to extreme heat loads. The paper aims to shed light on the strengths and weaknesses of different cooling methods, ranging from fundamental film cooling to advanced approaches like transpiration, effusion, and impingement cooling. Through a thorough review of experimental and numerical studies, this paper seeks to provide valuable insights into the capabilities and limitations of each technique in addressing the complex cooling challenges posed by modern gas turbine engines. Ultimately, the goal is to contribute to the development of more efficient and durable cooling solutions for these crucial engine components.

II. MOTIVATION OF USING COOLING TECHNIQUE

It is projected that fossil fuels will meet approximately 80% of the world's energy demands by 2035 [13-15]. However, this increased reliance on fossil fuels also brings greater responsibility, echoing the famous quote, "With great power comes great responsibility." The development of gas turbine engines has advanced significantly, but it has led to a corresponding rise in emissions. Aviation emissions have two significant effects: one pertains to local air quality, especially in proximity to airports, and the other relates to global climate change [16-21]. Aircraft exhaust accounts for approximately 70% to 80% of all NO_x emissions at airports. The primary pollutants released by airplanes include NO_x (comprising NO and NO_2), Unburned Hydrocarbons (UHC), Carbon Monoxide (CO), Sulfur Oxides (SO_x), and Particulate Matter (PM), primarily composed of smoke and soot [21]. Table 1 provides an overview of how these emissions impact human health [21,22].

According to Lee et al. (2021), the consumption of fuel by aircraft engines reached a staggering volume of over 1 billion litres per day over the period spanning from 2016 to 2019, prior to the onset of the global pandemic. During the process, they release 3.16 kg of carbon dioxide (CO_2), 1.23 kg of water vapor (H_2O), a maximum of 15.14 g of nitrogen oxides (NO_x), 1.2 g of sulphur dioxide (SO_2), and 0.03 g of black carbon (soot) per kilogram of fuel burned. The atmospheric interaction of nitrogen oxides results in the modification of the radiative equilibrium of

several gases, such as methane (CH₄), ozone (O₃), and stratospheric water vapor (H₂O). Consequently, these alterations have an indirect influence on the climate. According to Lee et al., (2009), the emissions other than carbon dioxide (CO₂) contribute to an extra net warming impact.

Table 1 Health impact of Jet Emissions [21,22]

Pollutant	Health Effect
Carbon Monoxide	Heart or respiratory disease
Nitrogen Dioxide	Respiratory infections
Sulfur Dioxide	Irritation to the eyes, nose, and throat
Unburned Hydrocarbons (Primary component of Volatile Organic Compounds or VOC)	Eye and respiratory tract infection
Particulate Matter (Smoke is a primary component of PM)	Aggravation of respiratory and cardiovascular disease

Reducing emissions from gas turbine engines can be accomplished by minimizing fuel consumption during flight. Achieving this involves elevating both the pressure and temperature within the combustion chamber. For example, as shown in Figure 2, the CO (Figure 2(a)) and UHV (Figure 2(b)) exhausted by the gas turbine engine was exponentially reduced as the temperature increased. However, this approach can have repercussions for the combustion chamber's longevity, particularly its walls or liner. Consequently, implementing effective cooling techniques becomes a critical aspect of gas turbine engine design. Numerous cooling methods have been developed to mitigate the excessive heat stress experienced by the combustion chamber liner. These methods include film cooling, effusion cooling, transpiration cooling, and impingement cooling. Additionally, thermal barrier coatings have been applied to the wall surfaces, which possess low thermal conductivity, aiding in the reduction of heat transfer to the liner wall.

III. FILM COOLING

When discussing film cooling, it represents the fundamental and straightforward technique for cooling the combustion liner. Film cooling is, in fact, a crucial cooling method not only for safeguarding the combustion liner but also for protecting other vital components within the gas turbine engine, including turbine blades, from heat-related damage [23]. The operational temperatures of gas turbine engines are steadily increasing and are expected to reach levels exceeding 2200 K soon, surpassing the melting point of most substrate materials [24]. Therefore, achieving effective thermal protection for the hot spots within gas turbine engines is paramount. Film cooling technology is employed not only for combustor liners [25-27] but also for cooling other components such as turbine components [28,29], guide vanes, blades [30-32], and

exhaust nozzles [33-35], highlighting its versatility. Besides that, film cooling also can help in diluting the high temperature of the air inside the combustion engine as high temperature led to an exponentially higher level of NO_x emissions as shown in Figure 2(c). Therefore, the air from film cooling was indirectly help in lowering the temperature inside the combustion chamber.

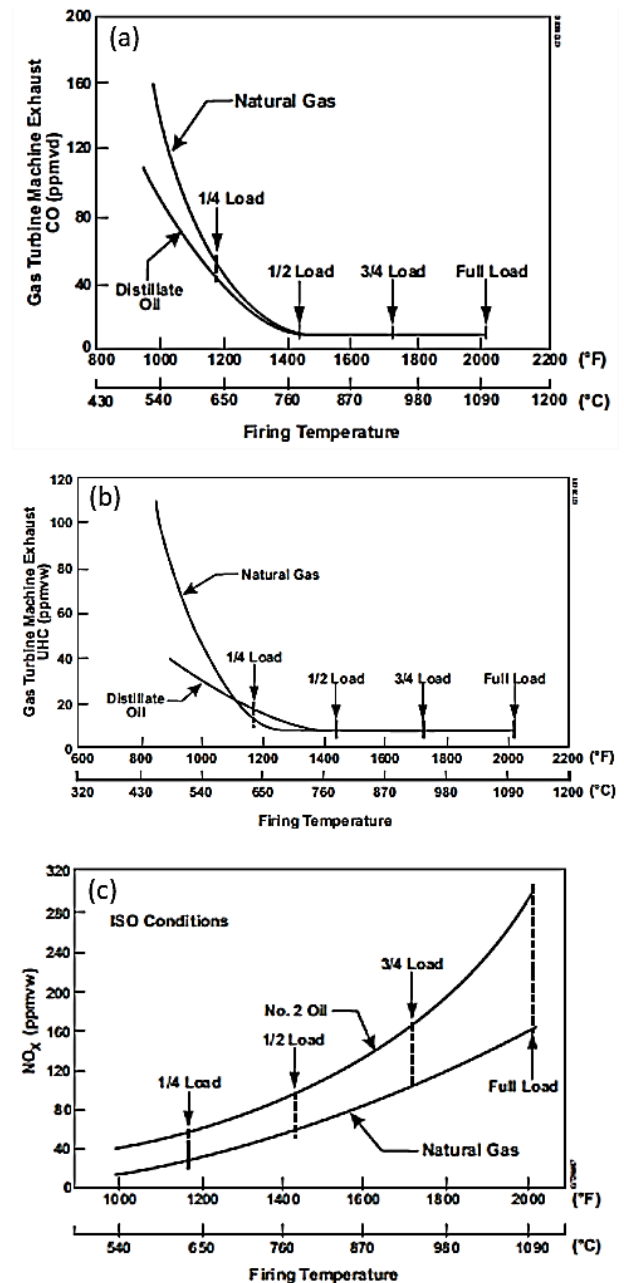


Figure 2 Effect of increasing temperature on Emission (a) CO₂, (b) UHC, (c) NO_x

Nevertheless, the film cooling technique consumes a substantial portion of the air directed from the compressor, typically around 70% to 80%, resulting in performance degradation. Consequently, there is a need for improvements that can meet the stringent thermal protection requirements of hot-section components while using less cooling air [24]. Film cooling is influenced by various factors, including the shape of the film cooling

hole, turbulence, Reynolds number of the mainstream flow, momentum ratio, density ratio, and blowing ratio between the cooling gas and the mainstream, among others. Of utmost importance within the film cooling technique are the blowing ratio, representing the dimensionless mass flux rate of the cooling gas, and the density ratio, which determines the dimensionless temperature of the cooling gas. These factors collectively determine the specific heat capacity of the cooling gas, which is pivotal in protecting hot components [36]. However, since in most cases of gas turbine engine was cooled using air, therefore, the density ratio was assumed to be equal to 1. Due to that, most of the film cooling was more focused on the effect of blowing ratio. Most of the time, for a simple cylindrical jet hole, the optimum blowing ratio was adjusted to be 1 but depending on the shape of the exiting cooling hole, the value might vary as shown in Figure 3.

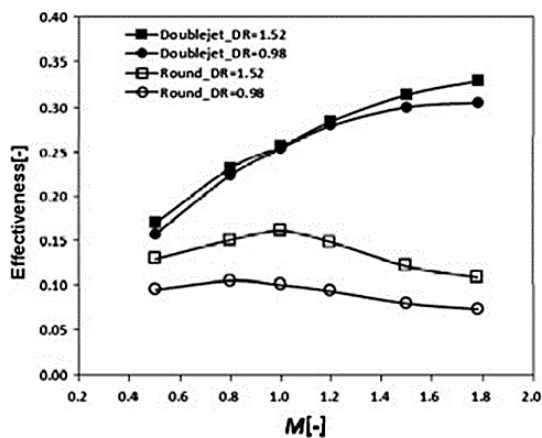


Figure 3 Film effectiveness of double jet and round hole at varied blowing ratio

The two-dimensional slot film cooling is often considered an ideal state-of-the-art technique. While it has been applied in numerous hot-section components of turbine engines, such as turbine end walls and combustor liners, its practical use is limited in many cases due to challenges in meeting thermal-mechanical requirements. Consequently, discrete film perforations have become the primary focus in practical applications. However, discrete-hole film cooling poses challenges as it frequently results in insufficient film coverage over the protected surface due to its inherent geometric characteristics. As a result, extensive research efforts have been undertaken in recent decades to identify effective methods, both passive and active, for enhancing discrete-hole film cooling. These holes have evolved from a simple circular hole to a more complex geometry design with the available of more advanced manufacturing techniques. These evolutions were done by changing some parameter of the hole which in some cases, new shape of the hole was produced. Even though, these evolutions seem promising, but there is some trade-off when some parameter was changed, for instant, the hole will yield a wider lateral spreading of the film cooling but a shorter film coverage downstream the flow which effect the film cooling effectiveness downstream the hole. This was then can be tackle with reduced the

distance between the holes or hole pitch. But when the holes were close to each other, indicate the increasing of hole number needed to cool down the desired surface. Based on these statements, the parameter of the hole design is dependent on one to another. There are no one absolute design that do not have flaws while giving some advantages.

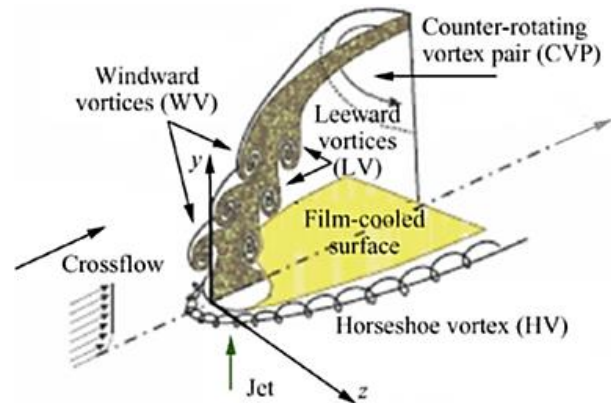


Figure 4 Schematic diagram of vortical structures of jet-in crossflow [24]

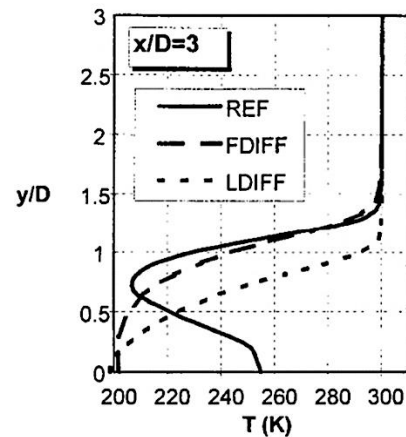


Figure 5 Centerline temperature profiles at $x/D=3$ for the REF, FDIFF, and LDIFF cases show the overall [44]

The primary concern in film cooling lies in the dynamics of jets in crossflow. Extensive studies have revealed that the interaction of discrete jets with the mainstream flow leads to the formation of intricate coherent vortex structures, as depicted in Figure 4. These structures include windward vortices (WV) at the leading edge of the jet, counter-rotating vortex pairs (CRVP) or kidney vortices within the jet, horseshoe vortices (HV) surrounding the jet, and leeward vortices (LV) at the jet's trailing edge [24]. Among these structures, the CRVPs have the most significant impact, substantially diminishing film cooling performance by promoting jet lift-off and penetration of hot gases. For instance, a study done by Hyams and Lylek [44], by changing the shape of the jet hole help in reducing the effect of CRVP and can improve the averaged heat transfer at the hole exits by

around 14% to 20% depending on the shape of the hole. The centreline temperature profiles in Figure 5 show that the coolant core remains close to the wall, in contrast to the lifting apparent in the cylindrical reference film-hole case.

IV. BLOWING RATIO

From the quantitative perspective, the determinative factor of the cooling performance is the coolant consumption, which can be defined as the blowing ratio (M) [24,37].

$$M = \frac{\rho_c U_c}{\rho_m U_m} \quad (1)$$

In cases with lower blowing ratios, no noticeable flow was detected, and the jet remained close to the wall due to the mainstream covering the upstream part of the hole, effectively pushing the jet towards the film-cooled wall (as illustrated in Figure 6(a)). Consequently, the fluid temperature predicted along the centreline closely matched the experimental data. Consequently, the CFD-predicted film effectiveness along the jet centreline also exhibited good agreement with the experimental results. At higher Mach numbers (M value), the influence of the mainstream flow on the jet flow was minimal near the exiting hole of the jet, resulting in significant penetration before the jet curved (as shown in Figure 6(b)). This is due to the higher momentum that the flow exiting the coolant hole are not affected by the cross flow of the mainstream up until the further downstream where the coolant flow has lost some momentum and it start to be affected by the mainstream flow and start to curve toward the surface.

It can be deduced that when the blowing ratio (M) is excessively high, there is a risk that the coolant jet flow may start to detach from the intended surface. In such cases, the protective film meant to shield the surface might prove insufficient in preventing the surface from heating up. El-Ganry et al., [38] conducted a CFD simulation, which successfully predicted the vertical extent of the film-affected zone but struggled to capture the vertical mixing in the wake region of the jet. This limitation made it challenging to define film effectiveness. This phenomenon can be explained by considering the presence of counter-rotating vortex pairs (CRVP), commonly referred to as kidney vortices. When the blowing ratio of the coolant jet is too high, often surpassing 1, it tends to adversely affect the effectiveness of film cooling, as the orientation of these vortices typically leads to the lifting of the vortex pair off the cooled surface, allowing hot gas to flow beneath, as illustrated in Figure 7(a) [39-41]. These effects have a detrimental impact on the cooling process. Hence, the primary means of enhancing film cooling lies in mitigating the presence of kidney vortices. This can be achieved by inducing what is known as an anti-kidney vortex pair, which redirects the detrimental velocity induction away from the cooled surface and transforms it into a beneficial induction toward the surface by generating a reverse-rotating kidney vortex pair. Furthermore, the counterproductive suction of hot gas

beneath the vortex pair is transformed into advantageous span-wise spreading of coolant, as depicted in Figure 7(b) [24,40,42].

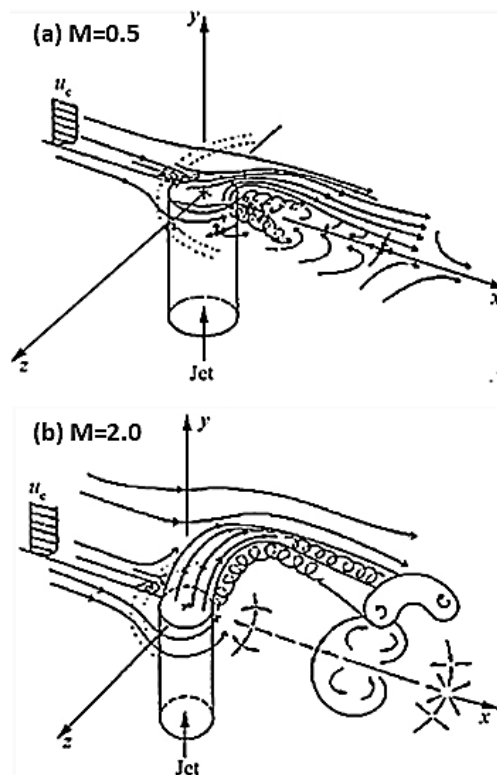


Figure 6 Blowing ratio effect on the crossflow structure [24]

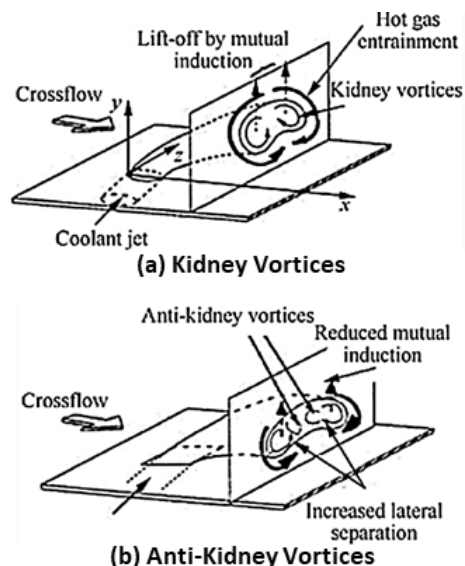


Figure 7 Schematic diagram of kidney and anti-kidney vortices [24]

According to Haven and Kurosaka [43], the anti-kidney vortex can be created by carefully crafting the film jet holes, which will aid in lowering the mutual induction

between the CRVP even the blowing ratio was high. This was then further explained by Hyams and Leylek [44] that besides the shape, the positioning of the hole also important to minimize the vortices lifting effect. But according to Bunker's assessment [45] of over 2,500 publications on film cooling, only around 50 of them particularly look at the impact of shape, expanded exit film hole aerodynamics, and thermal performance. Although there is now a lack of knowledge regarding the physics and parametric influence of shaped films holes, the acceptability of the technology is mostly based on the data from round film holes. These sorts of film holes are utilised wherever possible in the practise of cooling gas turbine engines due to the benefits of the shaped holes, which are genuine and considerable.

V. HOLE DESIGN

Advancements in the design of cooling holes have indeed demonstrated their ability to improve the effectiveness of film cooling. For instance, in the 1970s, research conducted by Goldstein et al., [46] revealed that fan-shaped holes enhanced the cooling capacity compared to traditional cylindrical holes. Fan-shaped holes introduce more geometric variables into the equation, including orientation positions corresponding to forward and lateral expansions, forward diffusion angles, lateral diffusion angles, and more. Even when applied to a flat surface, the intricate correlations required to predict the effectiveness of adiabatic film cooling with fan-shaped holes make them an ongoing focus of interest for researchers to this day [47-49]. Subsequently, the design parameters of film cooling holes have undergone numerous optimization efforts, considering both thermal and aerodynamic performance, with the hope of fully realizing the potential of this established technique.

To offer an overview of the ongoing development in innovative film cooling hole designs, Table 2, recreated based on the work of Zhang et al., [24], presents a concise compilation of research related to common-shaped hole film cooling over the past decade. It's worth noting that this list is not exhaustive, as shaped-hole film cooling has remained a prominent area of research in recent years. Nevertheless, this limited compilation captures the essence of advancements in shaped-hole designs. Based on the table, the design parameter such as the dimension of the hole will affect the performance of the film cooling technique.

Dimensions of the Film hole

The dimensions of the holes have a significant impact, particularly in shaping the final configuration of the hole. Initially, the most elementary form of the hole is circular or cylindrical in shape. However, as the dimensions of the hole are altered, the shape can accordingly transform, ranging from a basic elliptical shape to more intricate configurations like the fan-shaped hole depicted in Figure 8.

Altered hole designs, such as the fan-shaped hole, introduce a more complex set of geometric factors compared to the cylindrical hole. These factors encompass various aspects, including orientation positions corresponding to forward and lateral expansions, forward and lateral diffusion angles, and more. Even when applied to a flat surface, the precise correlation of fan-shaped holes continues to pique the interest of researchers who seek to enhance film cooling effectiveness. This underscores the ongoing optimization efforts, particularly for fan-shaped holes, which undergo multi-parameter optimization to fully exploit their latent potential, taking both aerodynamic and thermal performance into consideration.

Table 2 Selected research related to the common shaped-hole film cooling holes

Shaped hole type	Reference
Console	Liu et al., [50]; Yao & Zhang [51]; Yao et al., [52,53]; Pu et al., [54]; Wang et al., [55]
Combined Hole	Chang et al., [56]
Fan, Crescent, Louver, and Dumbbell-Shaped	Kim et al., [57]
Leaf-shaped	Lee & Kim [58]
NEKOMIMI (Cat Ears shape)	Kusterer et al., [59-61]
Cratered and trenched hole	Davidson et al., [62]; Kalghatgi & Acharya, [63,64]; Kim & Kim [65]; An et al., [66]; Feng et al., [67]
Bean, Clover, and Wintersweet	Yang et al., [68]
Sister shaped single hole (SSSH)	Khajehhasani & Jubran [69]
Tripod cylindrical hole	Ramesh et al., [70]; Chi et al., [71]; Ramesh et al., [72]
Round-to-slot hole	Zhang et al., [73]; Huang et al., [74]; Zhu et al., [75]
Horn shape	Zhu et al., [76]

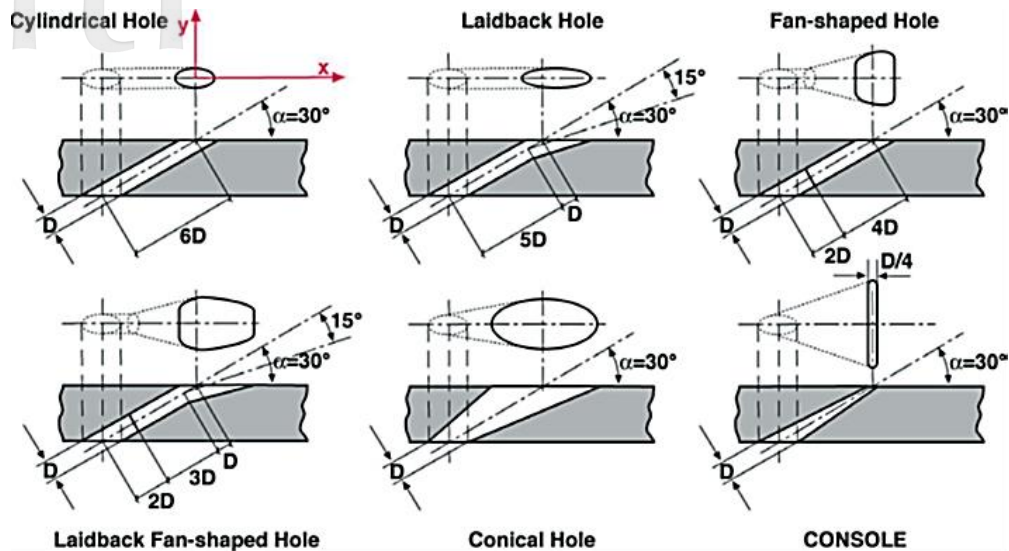


Figure 8 Basic designs of film cooling holes [77]

Table 3 Film cooling holes geometry [78]

Effect	Configuration	L/D	AR	P/D	C/D	β_{lat} (°)	β_{forw} (°)	γ (°)
L/D	A	11.5	3.5	6	0.49	6	2	0
	B	9.5	3.5	6	0.49	7	4	0
	C	7.5	3.5	6	0.49	7	11	0
P/D	D	11.5	4.2	4	0.65	4	8	0
	E	11.5	4.2	6	0.43	4	8	0
	F	11.5	4.2	8	0.32	4	8	0
C/P	G	11.5	2.5	6	0.31	2	4	0
	H	11.5	2.5	6	0.37	4	2	0
	I	11.5	2.5	6	0.39	4	0	0
	E	11.5	4.2	6	0.43	4	8	0
	K	11.5	4.2	6	0.57	7	2	0
	L	11.5	4.2	6	0.63	9	0	0
AR	M	11.5	3.5	6	0.43	4	4	0
	E	11.5	4.2	6	0.43	4	8	0
	L	11.5	4.2	6	0.63	9	0	0
	N	11.5	4.7	6	0.63	8	3	0
	E	11.5	4.2	6	0.43	4	8	0
Compound angle	K	11.5	4.2	6	0.43	4	8	45
	O	11.5	4.2	6	0.43	4	8	60
	P	11.5	4.2	6	0.43	4	8	45

For instance, Gritsch et al., [78] conducted research to identify the geometrical characteristics of film-cooling holes that significantly impact their effectiveness. These characteristics include hole length-to-diameter ratio (L/D), exit-to-inlet area ratio (AR), pitch, the ratio of hole exit width to pitch (C/P), and the compound angle of the hole, as illustrated in Figure 9.

A test matrix was developed, encompassing 16 distinct hole geometries, as presented in Table 3. Given that changes in one parameter often affect others, isolating these impacts has proven challenging. Therefore, the test matrix and corresponding hole geometries were thoughtfully selected to enable the discrimination of the effects of various geometric hole characteristics. The

results indicated that the geometry of the fan-shaped hole did not have any bearing on pressure losses, as measured by discharge coefficients.

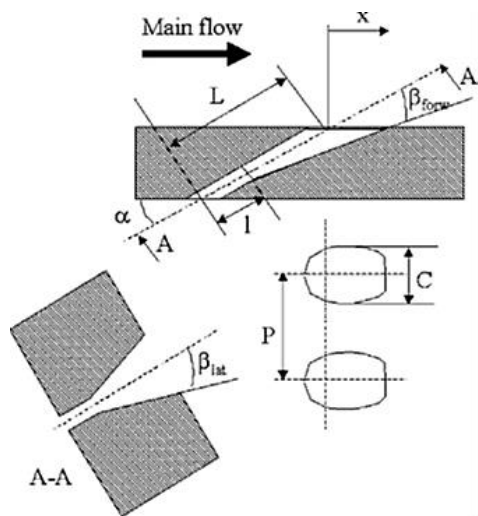


Figure 9 Film-Cooling Holes Geometry [78]

To provide a brief overview of the study's preliminary findings, it was observed that the film-cooling effectiveness remained consistent throughout the three L/D ratios studied in this study, namely $L/D=7.5$, 9.5 , and 11.5 . Given that the length of the cylindrical inlet portion remained consistent across all configurations, it can be concluded that the film effectiveness is not affected by the length of the hole diffuser section. The pitch-to-diameter ratio (P/D) serves as a metric to quantify the density of holes per unit span, as well as the cooling efficiency per unit span at a specific blowing ratio. Hence, it is unsurprising that the hole arrangement with a P/D ratio of 4 exhibits superior film-cooling performance when compared to configurations with P/D ratios of 6 and 8. Evidently, when the ratio of the pitch to the diameter (P/D) is equal to 4, the proximity of the holes is such that the effective utilization of the coolant is compromised. The area ratio, denoted as AR , is a quantitative measure that represents the ratio between the cross-sectional areas at the exit and intake of a hole. The parameter under consideration is believed to represent the capacity of the opening to facilitate the dispersion of the coolant within the fan-shaped region of the hole, thereby leading to a decrease in the momentum of the coolant. Reduced momentum results in reduced penetration into the primary flow, hence yielding enhanced film cooling efficiency. Therefore, higher aspect ratios (AR) suggest that the hole exhibits a greater degree of forward diffusion compared to a smaller AR ratio, resulting in improved film cooling efficiency. The use of a compound angle in cylindrical film holes has been seen to enhance the lateral dispersion of the coolant and mitigate the extent to which the coolant jets penetrate the primary flow. Consequently, there is an observed improvement in the effectiveness of film-cooling, although with the trade-off of increased heat transfer

coefficients resulting from heightened interaction between the coolant and the main flow.

Effect of length-to-diameter ratio

The length-to-diameter (L/D) ratio of film cooling holes used in the combustion chamber and afterburner liner of an aero engine typically falls within the range of 1 to 2, while for turbine blades, it exceeds 3. In literature classifications, cooling holes with $L/D < 3$ are categorized as short holes, while those with $L/D > 3$ are termed long holes. Secondary fluid emerging from long holes exhibits characteristics resembling fully developed turbulent flow in a pipe, whereas secondary fluid emerging from short holes leads to a jetting effect. To gain a deeper understanding of the cooling effectiveness of these long and short cooling configurations, Singh et al., [79] considered five values of L/D within the range of 1 to 5.

As depicted in

Figure 10, the far-field region demonstrates relatively consistent film cooling effectiveness for short holes, specifically when $L/D \leq 3$. However, for long holes with L/D ratios of 4 and 5, the film cooling efficiency varies significantly. An increase in the L/D ratio corresponds to an improvement in film cooling efficiency.

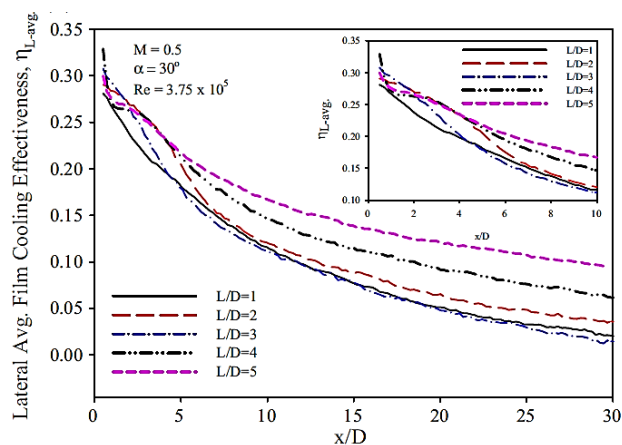


Figure 10 Lateral average film cooling effectiveness variation at investigated length-to-diameter ratios [79].

Conversely, the findings reported by Li et al., [80,81] exhibit a slight contradiction when compared to the results presented by Singh et al., [79]. In accordance with Figure 11, as the length-to-diameter ratio increased, the pattern of film cooling effectiveness often displayed a "V" shape. The highest film cooling values and minimal film jet lift-off were observed at an L/D ratio of 0.5. Notably, a strong lateral diffusion pattern was evident in the coolant, and the high-efficiency region exhibited an oval shape. This phenomenon is likely attributed to the interaction between the jet and crossflow, which enhances the dissipation of counter-rotating vortex pairs (CRVP). The coolant core exhibited a striped configuration, and lift-off occurred when the L/D was 2, resulting in reduced lateral diffusion and film coverage. For L/D values of 5, the jet initially lifted off and then reattached in the region between $x/D=3-5$.

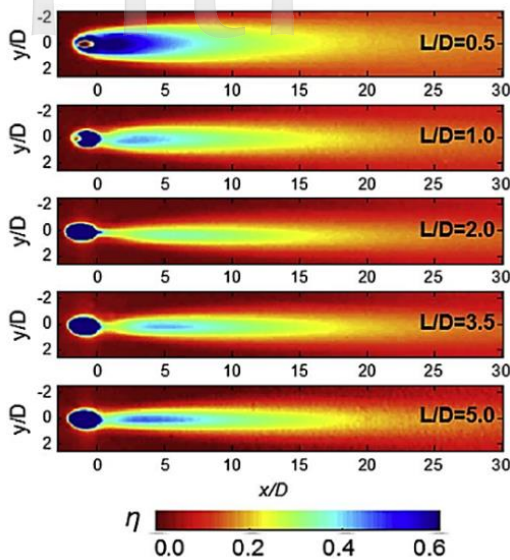


Figure 11 Film cooling effectiveness distribution for hole with varied length-to-diameter ratio, $M=0.8$ [80,81]

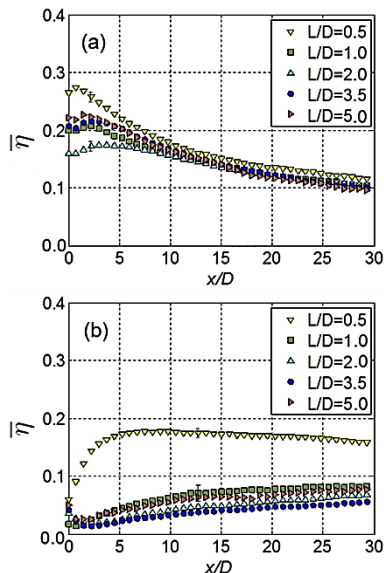


Figure 12 Laterally averaged film cooling effectiveness with varied L/D (a) $M=0.5$, (b) $M=1.5$ [81]

Furthermore, Figure 12 illustrates the film cooling effectiveness of a simple angle hole with different length-to-diameter ratios and blowing ratios, which has been laterally averaged. Figure 12(a) and Figure 12(b) illustrate that the influence of the ratio of hole length to diameter (L/D) on the effectiveness of film cooling primarily occurs in the downstream region of the hole up to $5D$. This impact is more pronounced when the blow ratio is low. Nevertheless, when considering the high blow ratio, the impact of the length-to-diameter ratio was shown to be considerable. The film with a length-to-diameter ratio (L/D) of 0.5 exhibited the highest film effectiveness. In contrast, the film cooling efficacy is found to be at its lowest when the length-to-diameter ratio (L/D) is equal to 3.5.

Furthermore, in another study by Li et al., [82], it was stated that the length-to-diameter ratio primarily influences the interaction between a jet and crossflow. A shorter L/D ratio intensifies turbulence near walls, resulting in higher heat transfer coefficients. As the L/D ratio increases from 0.5 to 3.5, the heat transfer coefficient progressively decreases by about 26% at exit of the hole area; however, as the L/D ratio rises from 3.5 to 5, it increases by around 13% at the hole exit area as shown in Figure 13. This behaviour is believed to be a consequence of a negative feedback loop between the increasing CRVP and the diminishing turbulence intensity in the jet core.

The slight variance in viewpoints between Singh et al., [79] and Li et al., [80-82] may be attributed to the subtle differences in the geometrical design of the cooling hole. In the studies conducted by Li et al., [80-82], the hole had a straight cylindrical shape with equal exit and inlet areas, resulting in an area ratio (AR) of 1. Conversely, in the study by Singh et al., [79], the cooling hole had different exit and inlet areas, with an AR of 3.5. This discrepancy in area ratios has an impact on the flow characteristics of the film and contributes to variations in the level of film cooling performance observed.

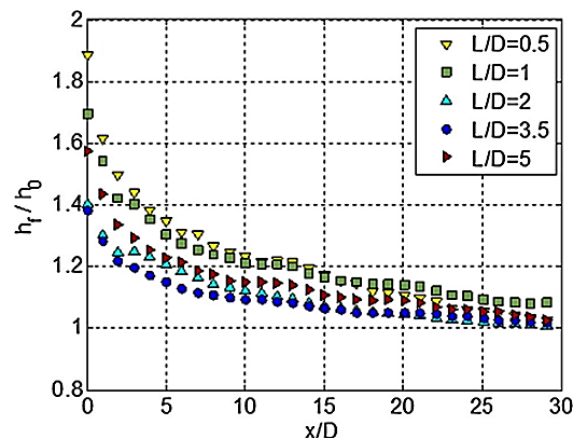


Figure 13 Spanwise averaged heat transfer coefficient h_f/h_0 distribution [81]

Effect of area ratio

The ratio of cross-sectional areas at the exit and inlet of the cooling holes is referred to as the area ratio, denoted as AR . This parameter is intended to characterize the hole's ability to disperse the coolant within the fan-shaped region of the hole, thereby reducing the momentum of the coolant. Lower momentum leads to less intrusion into the main flow and consequently enhances the film cooling performance. This type of hole design, often termed converging slot holes or console holes, has undergone extensive examination [50-52, 54,55].

Gritsch et al., [78] have noted that an AR exceeding 3.5 does not significantly affect film cooling effectiveness, suggesting that smaller ratios may yield different results. Smaller AR might lead to higher jet flow exiting from the coolant hole due to smaller exiting area especially the value below 1, which lead to higher penetration momentum into the mainstream flow for a similar blowing ratio. A more comprehensive investigation conducted by

Haydt et al., [83] considered three different area ratios ($AR = 2, 4, \text{ and } 6$). When the blowing ratio, denoted as M , was set at a moderate level of $M=1$, the contours of measured adiabatic effectiveness expanded as both the area ratio and the diffuser footprint width increased. However, there was a decrease in effectiveness near the trailing edge of the hole, likely attributable to mainstream ingestion and over-diffusion occurring in the diffusers of the larger area ratio holes (Figure 14(a)) where the mainstream flow overpowers the coolant flow. Nevertheless, the wider coverage of coolant on the end wall, especially downstream of the holes, offered by the larger breakout width of the larger AR hole diffusers largely mitigated the adverse mixing effects.

Different patterns emerge in the measured effectiveness contours at a higher blowing ratio of $M=3.0$

(Figure 14(b)). The contours narrow, indicating that the jet penetrates deeper into the mainstream. However, the larger area ratio holes behave differently in this scenario, suggesting that they experience less mainstream ingestion at higher blowing ratios. The adiabatic effectiveness contours at the highest blowing ratio of $M=6.0$ reveal that a small area ratio is a disadvantage as shown in Figure 14(c). Compared to Figure 14(b), the contours for $AR=2$ and $AR=4$ become narrower, while the $AR=6$ contours remain wide, with contour levels extending further downstream. Moreover, the effectiveness level at the trailing edge of the $AR = 6$ hole remains roughly the same across all cases, indicating that at this extremely high blowing ratio, over-diffusion and mainstream ingestion may not be occurring in the larger diffuser holes.

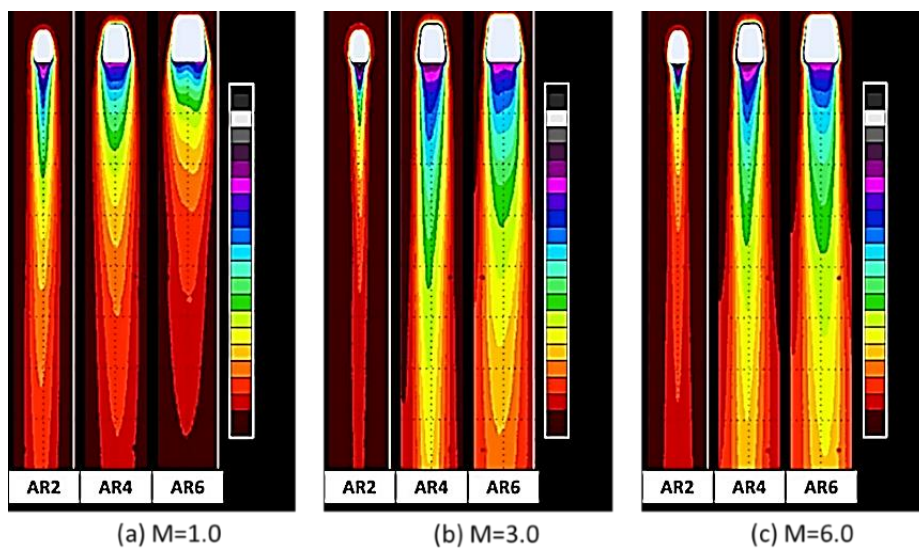


Figure 14 Contours of measured adiabatic effectiveness for all area ratios, at different blowing ratio [78]

This is supported by the research of Pu et al., [54], who conducted a study involving a row of converging slot-holes with two different area ratios (AR s), specifically $AR=0.69$ and $AR=1.38$. These holes were implemented upstream of a GE-E3 high-pressure turbine cascade liner to enhance film-cooling effectiveness in the end-wall leading-edge region and mitigate the influence of secondary vortices. Comparatively, the case with the smaller $AR=0.69$ demonstrated superior film-coverage performance, higher film cooling effectiveness, and greater effectiveness in weakening the secondary vortices compared to the larger $AR=1.38$ case. To enhance film cooling and reduce the impact of secondary vortices, a structure featuring a lower $AR=0.69$ and a 30° converging slot-hole is better suited for placement upstream of the cascade.

Other studies have investigated scenarios where the cooling holes become blocked. Figure 15(e) illustrates an axial cross-section of a film cooling hole, highlighting the accumulation of foreign material deposits within the hole. Such blockages can significantly affect cooling flow and efficiency [85]. This blockage situation can also be viewed as a reduction in the area ratio of the hole, as it alters the cross-sectional area at the inlet and exit of the hole.

Chen et al., [86] investigated various potential blockage scenarios affecting the film cooling characteristics of cylindrical and fan-shaped holes, as illustrated in Figure 15(a-d). These blockage scenarios are relatively common occurrences in cooling techniques, especially in the case of transpiration cooling. The results indicate that severe blockage ($H/D=0.75$) led to a significant reduction in the lateral-averaged film cooling performance for both cylindrical and fan-shaped holes, with decreases of approximately 97% and 27%, respectively. While it may appear that blockage negatively impacts film cooling effectiveness, it was observed that slight blockage (i.e., $H/D=0.5$), which reduces the exit hole area, increased the cooling efficiency of the fan-shaped hole by approximately 13%. Consequently, the deposition or blockage of the hole can either hinder or promote flow attachment on the surface, depending on the hole's shape. When considering hole shape, the fan-shaped hole exhibits greater tolerance to blockage compared to the cylindrical hole. Blockage alters the flow characteristics both downstream and within the hole. In the case of a blocked fan-shaped hole downstream, a phenomenon known as a "hairpin vortex forest" forms, featuring an increased number of hairpin vortices compared to the

unblocked configuration, as depicted in Figure 16. These large-scale coherent structures dominate mixing and dispersion. Conversely, the decline in cooling performance of the blocked cylindrical hole can be attributed to the strengthening of the head and horizontal legs of the hairpin

vortex. Additionally, near the wall, the streak structure, and several rows of smaller-scale hairpin vortices downstream of the blocked fan-shaped hole contribute to the enhanced efficiency of film cooling.

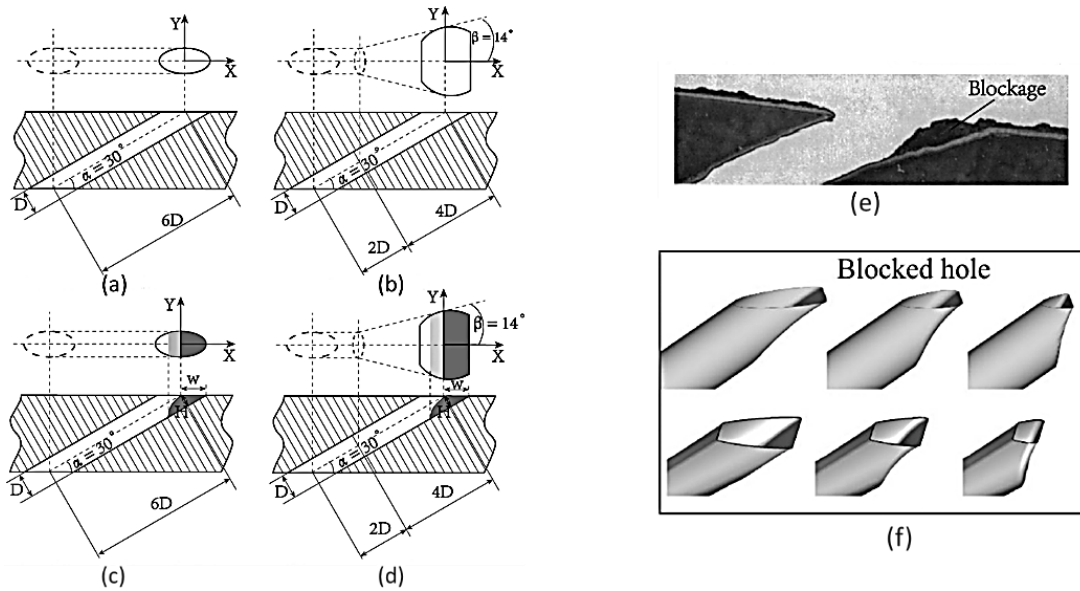


Figure 15 Sketch of blocked and unblocked film-hole geometries (a) cylindrical (b) fan-shaped (c) blocked cylindrical (d) blocked fan-shaped (e) micrograph of blocked film cooling from Bogard et al., [85]

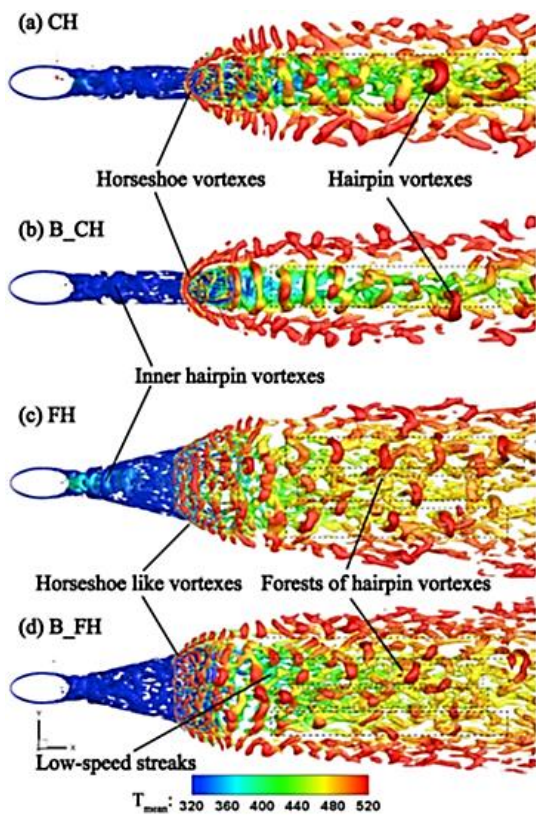


Figure 16 Instantaneous coherent structures inside and downstream of the film cooling tube [86]

Effect of pitch-to-diameter ratio

The gap between holes, commonly referred to as the pitch (P), can also have a significant impact, particularly on flow propagation and its influence on film coverage. Researchers often consider a pitch ranging from 3 to 8 holes diameters, as it has been observed to provide optimal coverage on the intended surface. A smaller gap or pitch results in a larger coverage area, and this doesn't solely depend on the hole diameter since individual jets can merge downstream, covering a larger surface area. Conversely, if the pitch is too large, the covered area will be determined by the hole diameter because there is no flow interaction between neighbouring holes [87].

A study conducted by Liu et al., [88] extended the pitch-to-diameter ratio (P/D) to 5 and 8 for cylindrical and laid-back holes. Figure 17 shown the distribution of film cooling effectiveness for the four test models at a blowing ratio of $M=0.7$ and 2.0. Under conditions of a small blowing ratio of $M=0.7$, the trajectory of jets in all four leading edge models exhibits a high degree of alignment with the mainstream direction. Furthermore, the jets effectively attach to the wall surface. As the blowing ratio is increased, the trajectory of the jet from the second-row hole exhibits a steady deviation towards the spanwise direction. Conversely, the jet originating from the first-row hole mostly flows in the spanwise direction. When the blowing ratios exceed 1, the jets detach from the surface of the model due to the presence of significant exit momentum. Additionally, the effect region of the jets expands because of the high jet flux.

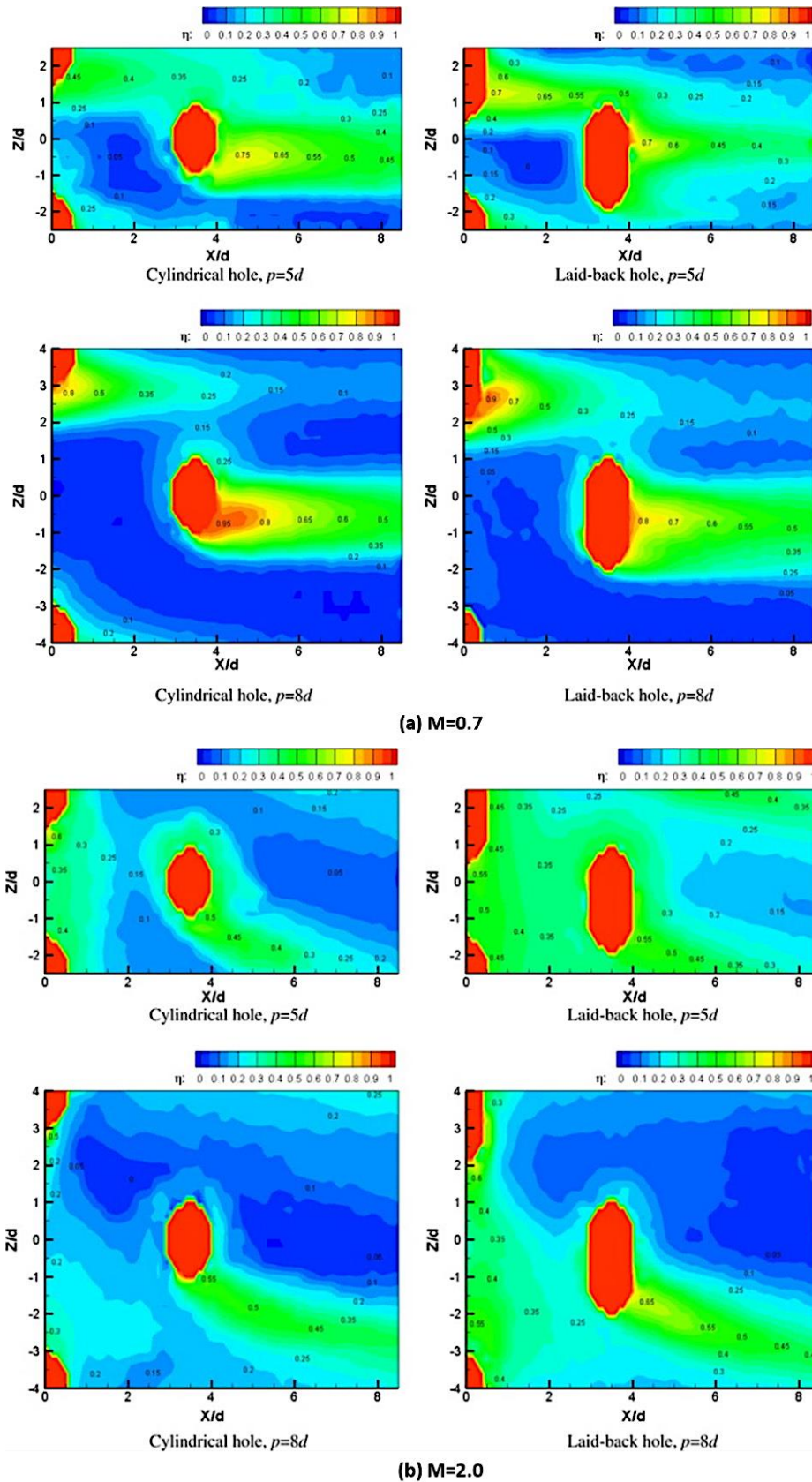


Figure 17 Distributions of local film cooling effectiveness under varied blowing ratio [88]

The expansion of film coverage can have a positive impact on a wider range of geographical areas. In the case

of models with a ratio of $p=5d$, the film covering performances of laid-back holes exhibit a level of

similarity to that of cylindrical holes when subjected to low blowing ratios. However, if the blowing ratio is increased, the performance of film covering by the laid-back holes improves progressively. The laid-back orifices yield an approximate 55% enhancement in the average film cooling effectiveness at a Mach number of 2. The intensity of flow interaction is greater in the $p=5d$ cases compared to the $p=8d$ cases due to the presence of a narrower hole-to-hole spacing. The lower jet's coverage

between the first and second rows is significantly expanded because of the upper jet's exertion of pressure. In models where the ratio of hole pitch to diameter is 8, the superiority of laid-back holes in enhancing film cooling effectiveness is particularly pronounced in the upstream region located between the first and second rows, as compared to cylindrical holes. In contrast to the $p=8d$ models, the $p=5d$ models exhibit a significantly greater proportion of film coverage in the area.

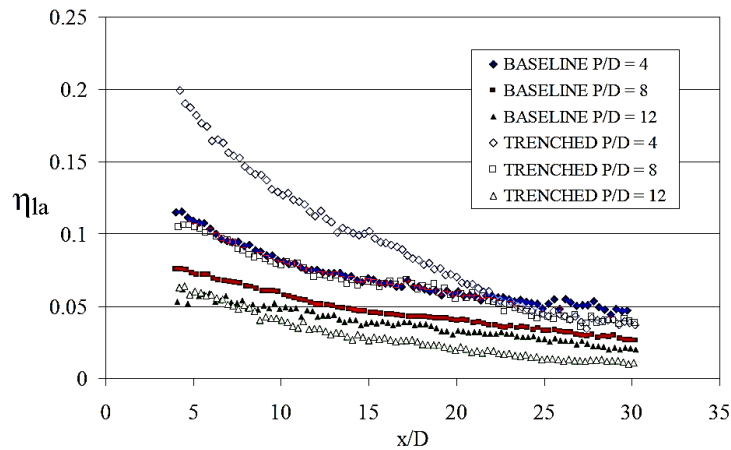


Figure 18 Span-wise averaged effectiveness for all cylindrical [89]

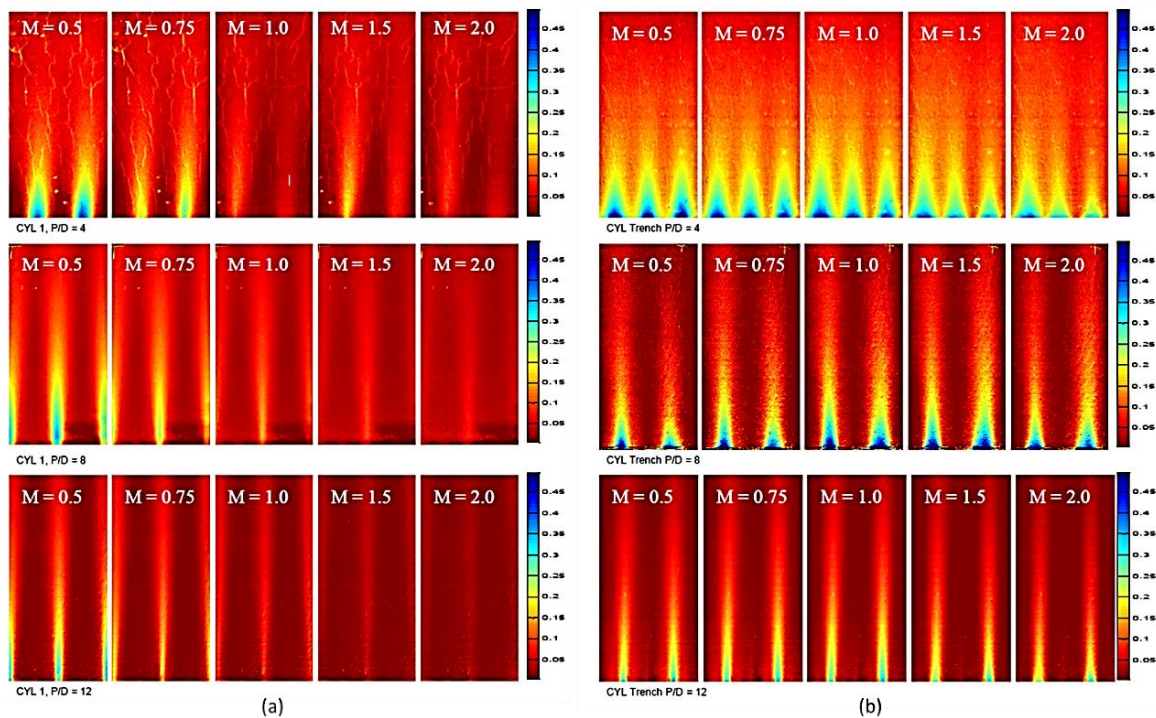


Figure 19 Film cooling effectiveness downstream of cylindrical holes (a) baseline (non-trenched)

A broader range of pitch ratios, spanning from $4D$ to $12D$, was examined by Zuniga and Kapat [89] in a study involving a single row of cylindrical holes positioned within trenches. Additionally, a flat test plate was employed as a reference baseline for the experiments. Flow interaction between neighbouring holes becomes particularly noticeable at low blowing ratios, such as 0.5.

However, in the case where the pitch was set at $4D$, the flow managed to cover a substantial downstream area even with a high blowing ratio, as illustrated in Figure 19(a).

This phenomenon did not occur with larger pitch values, especially $12D$. This behaviour arises because when the pitch is optimally close, the flow interaction between the holes generates vortices or turbulence that

aids in the recovery of flow from severe lift-off events. Hence, for a $4D$ pitch, there is still some downstream coverage of the film.

This situation improves further when the holes are embedded within trenches, resulting in a broader covered area, particularly with a $4D$ pitch as shown in Figure 19(b). Even with an increased blowing ratio of 1 or 2, there is no reduction in film coverage. This could be attributed to the trenches reducing the momentum of the coolant jet as it exits the holes, causing less penetration into the mainstream flow and minimizing the likelihood of flow being lifted off from the surface. Although the flow interaction is less noticeable in the case of an $8D$ and $12D$ pitch, the wider film coverage compared to a flat surface demonstrates that interaction does exist but on a smaller scale.

For instance, the coverage pattern for the trenched hole with an $8D$ pitch resembles that of a flat hole with a $4D$ pitch, as shown in Figure 18. This suggests that

trenching the holes array may reduce the number of required holes, a modification that will be discussed further later.

Effect of Compound Angle

Compound angles are frequently utilized in the cooling mechanisms of high-performance gas turbine engines. When it comes to film cooling, a compound angle injection hole is typically characterized by having two injection angles, as depicted in Figure 20. The inclination angle (α) is the angle between the injection vector and its $x-z$ plane projection, while the orientation angle (β) is defined as the angle between the streamwise direction and the injection vector's $x-z$ plane projection [90,91]. In the compound angle orientation system, a spanwise momentum component is introduced into the coolant. Consequently, compound angle holes offer more even film coverage in the spanwise direction.

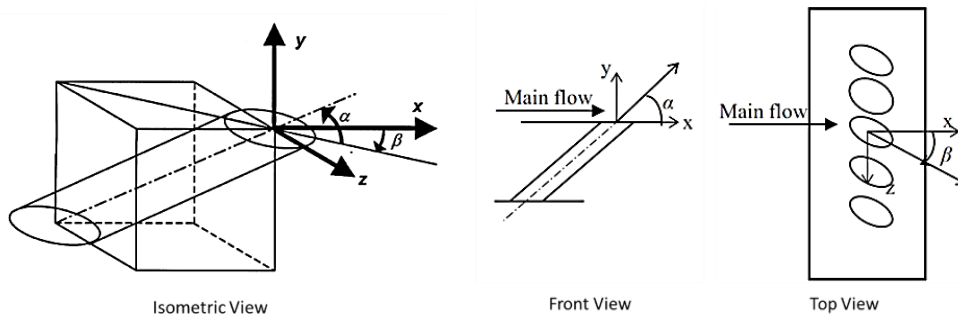


Figure 20 Configuration of compound angle injection [90,91]

In contrast to the simple angle injection system (where $\beta=0$), the counter-rotating vortices that are typically observed tend to merge into a single, robust vortex as the orientation angle increases. The strength of downstream secondary flow is significantly influenced by the velocity ratio [92].

Lateral jet injection offers a larger jet profile size and improved coolant coverage while keeping manufacturing costs relatively low. Previous researchers have conducted

numerous investigations to gain a deeper understanding of the flow physics mechanism involved in compound angle film cooling.

A detailed analysis conducted by Hyams and Leylek [44] focused on multiple hole configurations, including the effects of α and β angles in film cooling, which refer to forward and laterally diffused holes, as depicted in Figure 21.

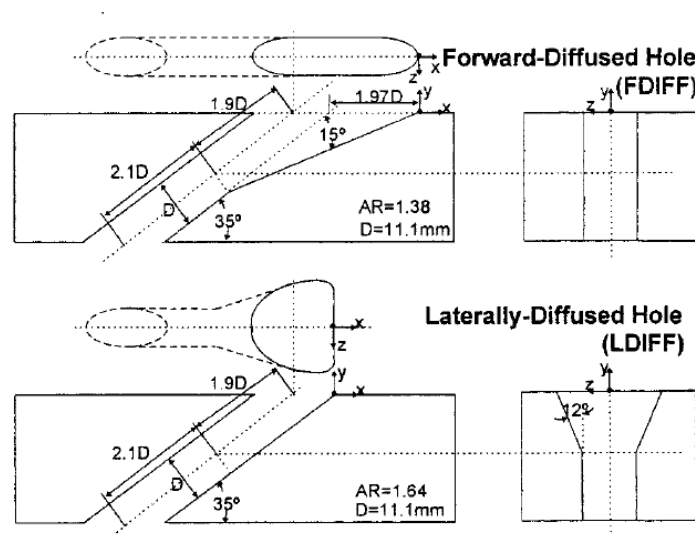


Figure 21 Forward and laterally diffused holes configuration [44]

The distributions of adiabatic cooling effectiveness and heat transfer coefficient on the cooling wall are significantly influenced by the vortex structures downstream of the jet. This implies that changes in α and β angles will impact the flow characteristics of the hole.

For instance, Figure 22 illustrates the effect of reducing the exiting flow α angle on aligned vorticity. A decreased α angle causes the jet stream to angle downward, reducing its contribution to aligned vorticity and allowing the mainstream flow to pass beneath it. Conversely,

increasing the α angle (as shown in Figure 22(b)) makes the jet flow stay closer to the surface without allowing the mainstream to pass under it.

Similar logic applies to variations in the lateral direction angle, β . However, one advantage of changing the lateral angle (β) is that laterally diffused film holes provide the best coverage and highest effectiveness. Forward diffused film holes perform well along the centreline but lack lateral spreading capability.

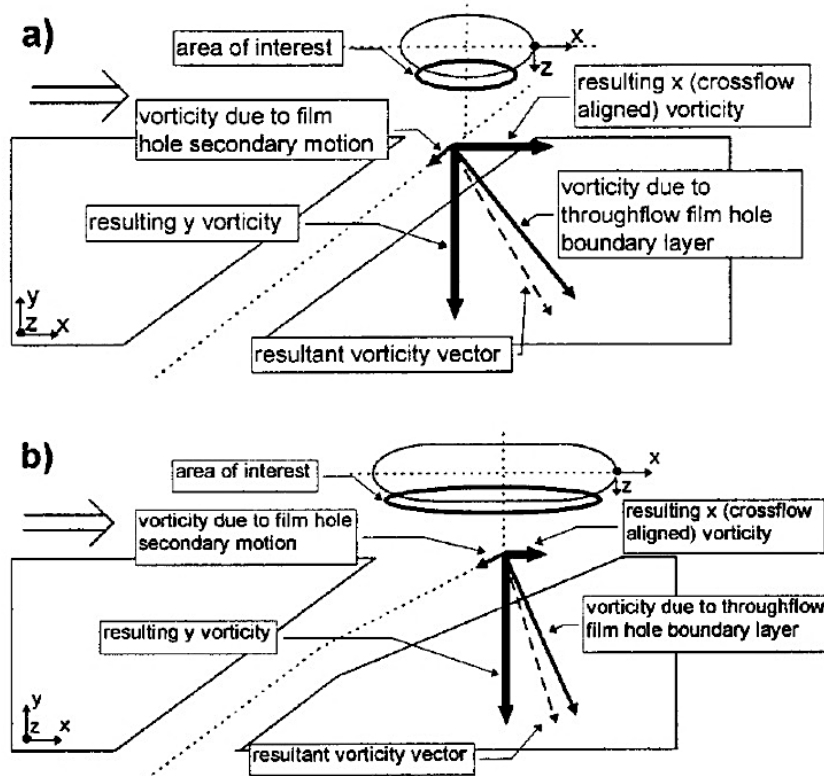


Figure 22 The effect of decreasing exiting flow α angle on aligned vorticity [44]

A similar phenomenon was observed by Aga and Abhari [93], who conducted a study involving an increase in the β angle value from 15 to 60 and 90 degrees. While high coolant effectiveness was observed near the hole, it did not extend significantly downstream of the stream. However, when the β angle value was increased from 15 to 90 degrees, the film managed to cover a larger surface area, as depicted in Figure 23.

This can be explained by the formation not only of vertical momentum in the jet stream but also of lateral momentum resulting from the interaction between the mainstream flow and the coolant jet flow. These two forms of momentum combine to create a single vorticity region that spreads over a broader lateral extent, no longer confined by the narrow trajectory of the hole diameter.

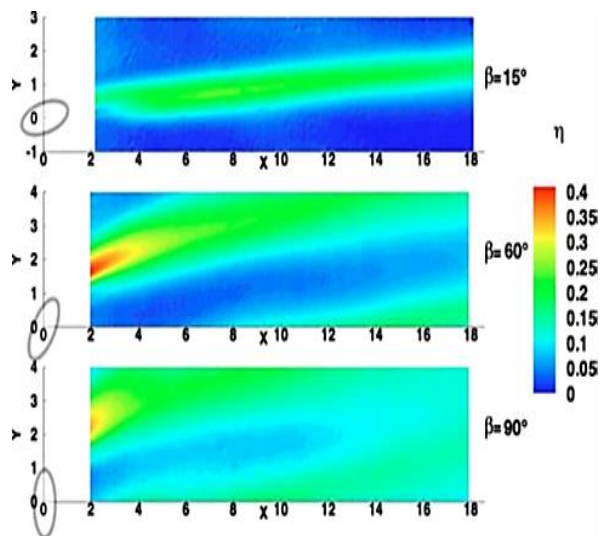


Figure 23 The adiabatic effectiveness contour for different β value [93]

Another way to explain this is that, with a β angle of 90 degrees, when the jet exits the hole, its trajectory can be divided into a vertical component and a lateral component. The vertical component attempts to penetrate perpendicularly into the mainstream, creating a vorticity region near the downstream of the hole. Meanwhile, the lateral component tries to penetrate to the side of the hole, generating vorticity on the hole's side. When these vorticity regions from the side and downstream of the hole merge, they produce a larger film coverage compared to when β is 0 degrees, causing the ejected flow to align with the mainstream flow direction.

Another study conducted by Li et al., [81] involved a comparison of film cooling effectiveness between holes with only streamwise angles and those with compound angles. In the initial part of the study with an L/D ratio of 0.5 (Figure 24(a)), the film effectiveness contours for both simple and compound angle holes appeared similar. This similarity may be attributed to the jet flow not being fully developed, indicating that the momentum generated for lateral penetration was insufficient. Consequently, the compound angle had no discernible impact on the jet, and

the exit jet direction was nearly identical to that of the simple angle hole.

However, when the blowing ratio was significantly increased to 0.8 and 1.5, the contour for the simple angle hole began to exhibit necking near the downstream of the hole, suggesting flow lift-off. In contrast, for the compound angle hole, the flow remained attached to the surface, indicating that the compound angle had the effect of suppressing jet blow-off at low L/D ratios and high blowing ratios.

In the second part of the study, where the L/D ratio was increased to 3.5, the film effectiveness contours for both simple and compound angle holes became more distinct even at lower blowing ratios, as shown in Figure 24(b). The compound angle hole began to exhibit slightly extended film coverage, surpassing the diameter of the hole, in contrast to the simple angle hole. As the blowing ratio increased, the jet flow began to detach further from the surface due to lift-off events, as the flow had become fully developed, signifying higher momentum to penetrate the mainstream flow. However, since the compound angle provided both lateral and vertical momentum, the flow managed to recover from severe lift-off events.

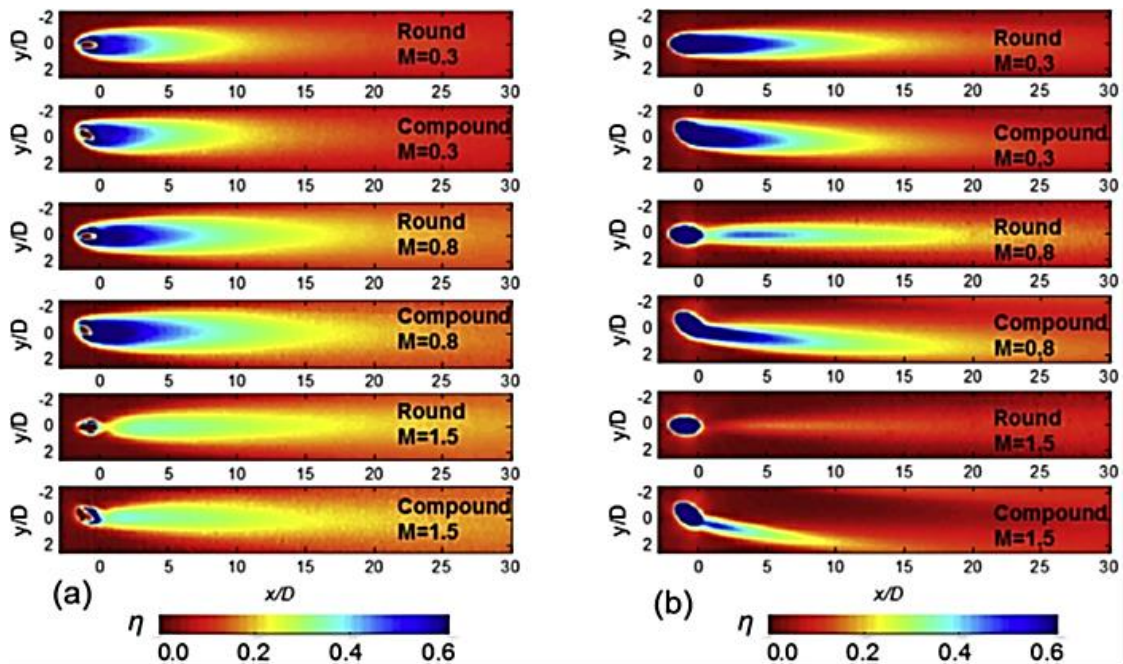


Figure 24 Film cooling effectiveness distribution for simple angle hole and compound angle hole with (a) $L/D=0.5$ and (b) $L/D=3.5$ with varied blowing ratio [81]

VI. UNIQUE SHAPE OF FILM COOLING HOLE

The evolution of film cooling hole designs extends beyond conventional shapes, with some unique configurations developed to address limitations unaddressed by multi-parameter optimization methods. Inspiration for these unconventional shapes often draws from nature, such as cats. Many of these novel hole designs result from the fusion of Double-Jet Film Cooling (DJFM) and fan-shaped holes, a combination known to

yield superior film effectiveness compared to traditional cylindrical holes.

Double-jet film cooling

The operation of DJFM is quite straightforward, involving the introduction of a secondary injection jet to generate counter-rotating vortices in relation to the primary injection jet [94]. The hole arrangement for DJFM is illustrated in Figure 25, typically with the secondary hole designed to mirror the first hole configured with a compound angle, β . This compound angle has been proven

to reduce the likelihood of lift-off events, even at high blowing ratios.

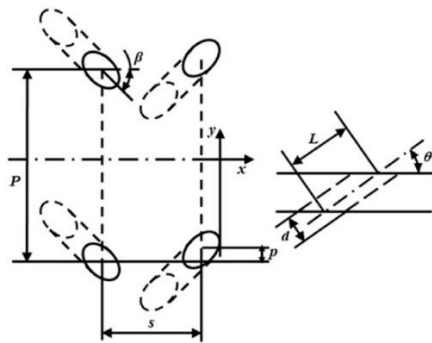


Figure 25 Double jet film cooling holes geometries [104]

Furthermore, DJFM has demonstrated the ability to provide greater downstream film coverage compared to a single hole with a similar compound angle because both holes in DJFM interact, generating larger counter-rotating vortices. This illustrates the principle that two holes are better than one. Although DJFM is conceptually simple, hole arrangement still requires consideration of various parameters, including blowing ratio [95,96], density ratio [97], compound angle [96, 98], mainstream angle of attack [99,100], pitch distance [98], streamwise distance [101,102], and spanwise distance [103,104], similar to that for a simple cylindrical hole.

Nekomimi type hole (Cat's ear shaped hole)

Nekomimi-shaped holes are crafted by carefully integrating both holes of DJFC while maintaining the configuration depicted in Figure 26.

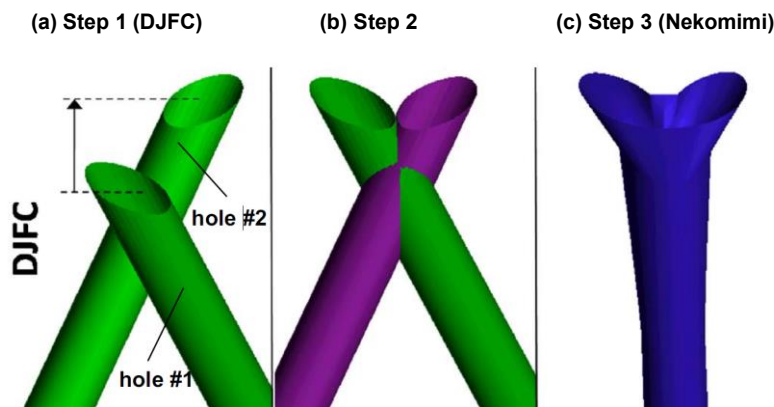


Figure 26 Nekomimi design concept [59-60, 105]

The process involves moving the holes closer to each other until they overlap (Step 1), subsequently merging the overlapping holes (Step 2), and replacing the supply hole with a single cylindrical hole, supplemented by a small diffuser (Step 3). This results in the exit of the combined

hole having a more refined geometric shape, as depicted in Figure 27. The term "Nekomimi," derived from the Japanese word for "cat ears," was chosen to describe this geometry because the final shape of the combined hole's exit now resembles a shape with two ears [59,105].

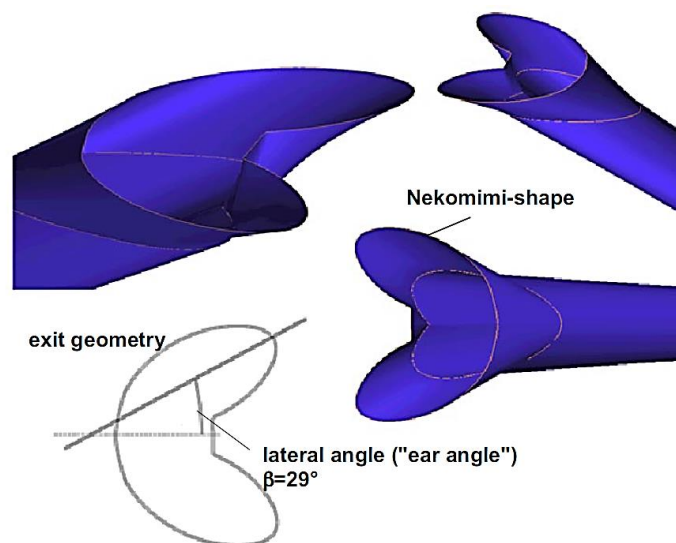


Figure 27 Exit shape of Nekomimi configuration [105]

As indicated by Kusterer et al., [105], the Nekomimi hole design demonstrates the ability to achieve notably high cooling effectiveness, particularly in the vicinity of the hole's centreline, as illustrated in the contour shown in Figure 28. Additionally, Nekomimi holes generate a larger lateral extension of film coverage compared to conventional hole shapes. This suggests that Nekomimi

holes not only deliver high film cooling efficiency, which matches or even surpasses that of shaped holes like fan-shaped holes, but also offer greater lateral film coverage, resembling the performance of holes designed with a compound β angle, which is typically lacking in terms of film efficiency.

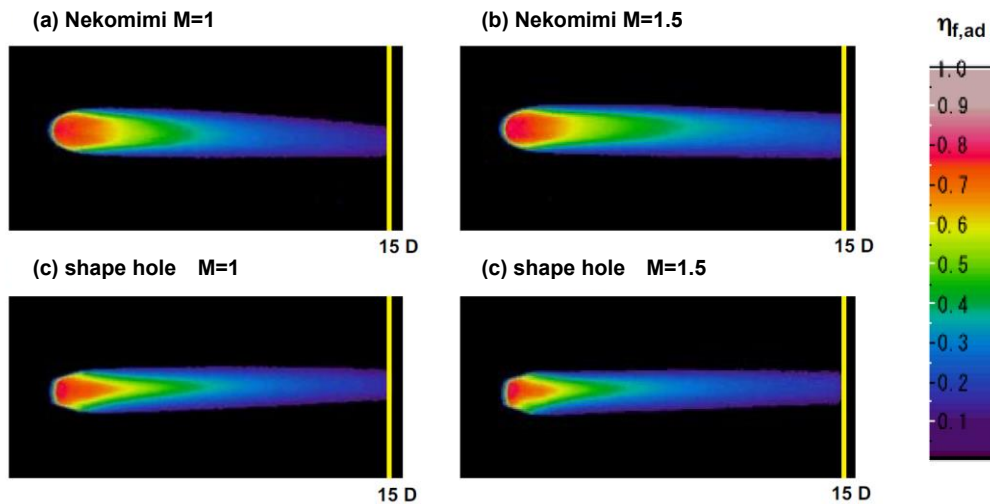


Figure 28 Measurement result of adiabatic film cooling effectiveness [105]

From the perspective of the blowing ratio, once again, Nekomimi holes demonstrate their superior performance. They exhibit an increase in film cooling effectiveness rather than the decrease observed in shaped holes when the blowing ratio is raised from $M=1.0$ to 1.5 . In the case of shaped holes, there is a lift-off phenomenon where the jet leaving the hole possesses high momentum and penetrates too deeply into the mainstream, resulting in detachment from the desired surface as the blowing ratio increases. This illustrates that Nekomimi holes effectively minimize the occurrence of lift-off events as the blowing ratio increases, contributing to more efficient cooling performance. This was due to the formation of anti-kidney vortices as shown in Figure 29. In Figure 29(a), it can be shown that at the location where $x/D=7$, the secondary flow vectors provide visible evidence of the presence of anti-counter-rotating vortices, also known as anti-kidney vortices, in the computational analysis. The prevention of main air penetration beneath the secondary air jet, also known as the "cooling jet" in real settings, is attributed to the direction of their rotation. Consequently, the occurrence of an air jet lift-off effect is averted. In addition, the jet is propelled in the direction of the wall's lower side, and the secondary air is likewise dispersed laterally, as evidenced by the temperature colour scheme. Subsequently, the lateral distribution is constrained by the obstructive influence exerted by the adjacent jets, resulting in a further amplification of the flow's swirling motion. This phenomenon reinforces the intensity of the shear-layer vortices, which are also observable beside the secondary air jet. The subsequent progression of the secondary vortices is observable in Figure 29(b-c). The magnitude of the vortices diminishes. However, the presence of the ACRV remains distinctly observable at the

location corresponding to $x/D=20$. The temperature distribution indicates that the secondary air jet maintains contact with the wall without experiencing lift-off. Based on the numerical computation, it can be asserted that the enhanced cooling effectiveness observed in the $M=1.5$ case, in comparison to the other configurations, is mostly attributed to the secondary flow influence of the ACRV.

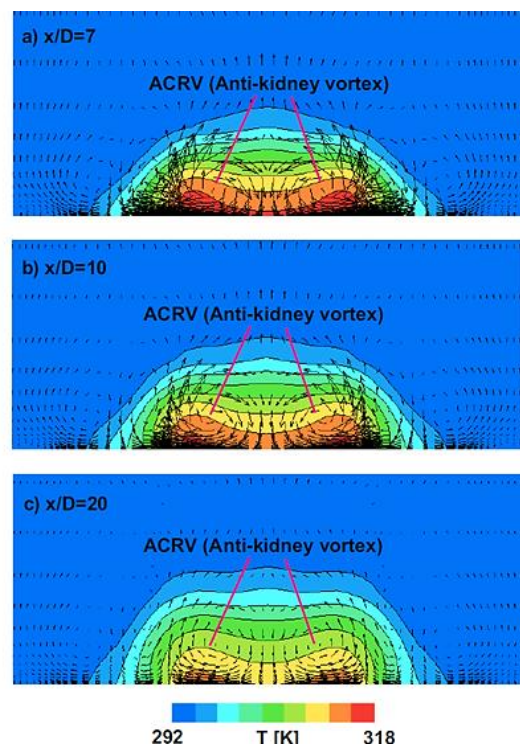


Figure 29 Temperatures and Secondary flow vectors for Nekomimi configuration at $M=1.5$ [105]

In comparison to other hole configurations, DJFC exhibits the most stable film efficiency. It doesn't experience as severe a reduction compared to the other hole configurations. The DJFC arrangement maintains high average values downstream of $x/D=12$ for $M=1.5$ and downstream of $x/D=10$ for $M=1$, whereas most other holes exhibit an exponential decrease in efficiency. This stability in DJFC performance may be attributed to the separated inlet of the DJFC, which provides a more consistent jet flow with less disturbance from the mainstream flow compared to other holes.

When the results are presented in the form of a plot and compared to other hole configurations, as depicted in Figure 30, several noteworthy insights can be gleaned. The Nekomimi hole outperforms all other hole configurations in terms of average adiabatic film cooling effectiveness, including its precursor, the DJFC hole. However, it's worth noting that the Nekomimi hole experiences a significant reduction in efficiency far downstream from the hole, a phenomenon also observed in other hole configurations, particularly at $M=1$. This reduction was anticipated, as lift-off events are likely to occur in the far downstream region of the hole.

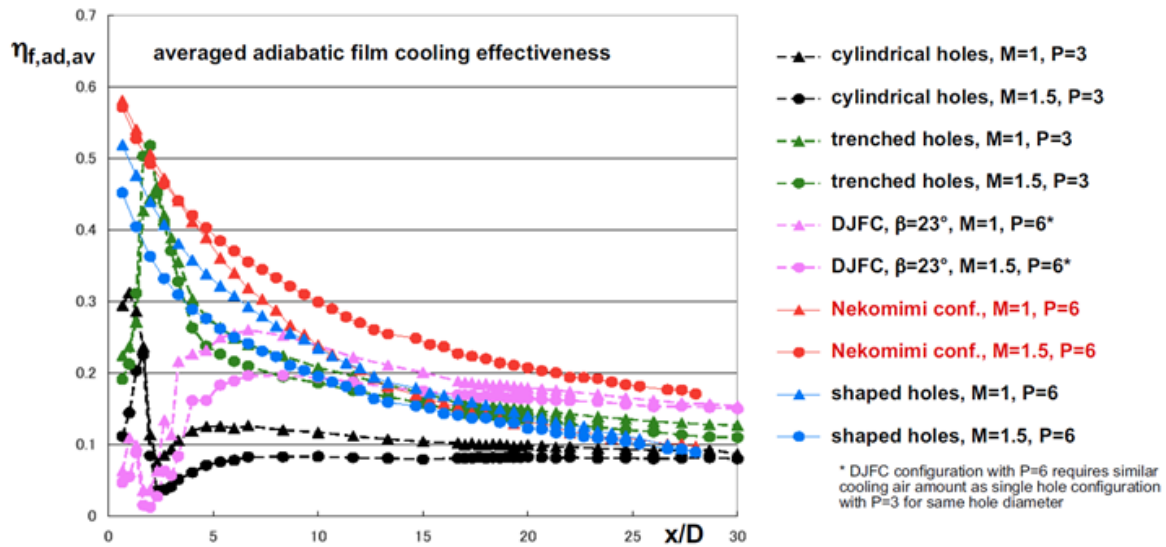


Figure 30 Averaged measurement of adiabatic film cooling effectiveness [105]

For the trrenched hole configuration, at both blowing ratios of 1 and 1.5, high film efficiency is achieved, especially inside the trench. However, this efficiency diminishes as it propagates in the negative direction further downstream, primarily due to the occurrence of lift-off events.

Table 4 Combination of Parameters by Kusterer et al., [60]

Configuration	β (°)	δ (°)	Hole Height Ratio H_c/H
Basic Geometry	29	5	0.5
Variation 1	32	10	0.5
Variation 2	32	7.5	0.75
Variation 3	32	10	0.625

In other studies, Kusterer et al., [60-61] conducted modifications to further enhance the optimization of the Nekomimi-shaped hole. This was achieved by investigating the influence of each fundamental configuration parameter on film cooling effectiveness and the structure of the jet vortex. Subsequently, combinations of parameter variations were explored with the aim of

synergizing the advantages of individual parameter adjustments to create hole configurations that would excel even more in film cooling. Table 4 presents the combinations of parameters that were examined by Kusterer et al., [60].

Figure 31 provides an overview of the various Nekomimi configurations studied, illustrating how parameter variations significantly impacted the shape of the holes.



Figure 31 Nekomimi configurations illustration [60]

The experimental and numerical results regarding film cooling effectiveness for both the basic Nekomimi hole and its variations are presented in Figure 32, along with results for simple cylindrical and shaped holes, all at

a blowing ratio of $M=1.5$. It is evident that the simple cylindrical hole lags behind the other hole designs in terms of film cooling efficiency, despite its higher blowing ratio. Variation 3 of Nekomimi, in the experimental results, demonstrates approximately a 17% improvement compared to the basic Nekomimi hole and a substantial 60% improvement compared to shaped holes.

On the numerical side, the results show even more significant enhancements for the Nekomimi hole and its improved variations. In comparison to the basic Nekomimi hole, variations 1, 2, and 3 exhibit enhancements of approximately 43%, 17%, and 35%, respectively. However, there is a noticeable difference between the

experimental and numerical results observed for variation 3. This discrepancy may be attributed to the flow distribution characteristics near the holes. In the experimental approach, it could be assumed that the enhancement in film cooling effectiveness was primarily due to lateral diffusion effects rather than improved anti-kidney vortex structures. Consequently, the actual improvement in cooling performance falls short of expectations. Further investigations are required to ascertain the reasons behind the variation in flow distribution inside the holes in both numerical simulations and experimental conditions.

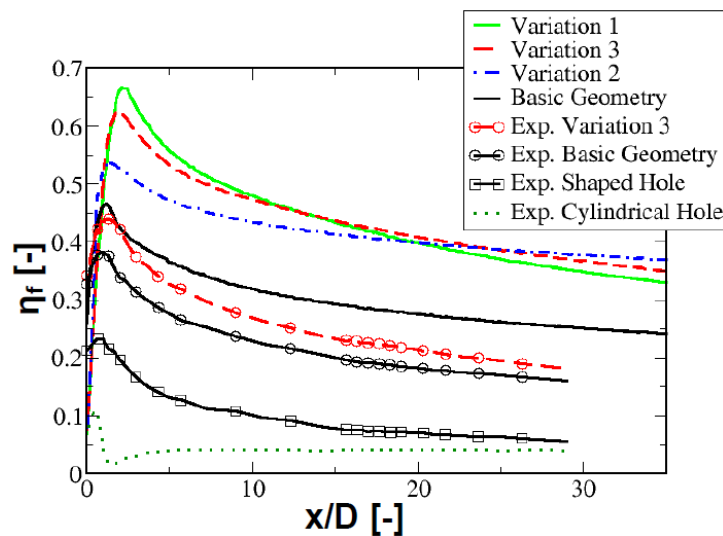


Figure 32 Adiabatic film cooling efficiency for the experimentally studied configurations as well as the numerical findings of the illustrative investigated configurations at a blowing ratio of $M=1.5$ [60]

VII. ADDITIONAL FEATURE AROUND THE FILM COOLING HOLE

The progression of film cooling techniques in gas turbine engines has extended beyond the design of film cooling holes. Numerous studies have explored additional features or geometric modifications around the holes that alter the interaction between the mainstream flow and the coolant flow. These modifications include the placement of vortex generators within each hole and the creation of a trench around a row of holes.

Vortex generator/ Ramp

As depicted in Figure 33, when the boundary-layer flow encounters a backward-facing step, it divides and creates a recirculation zone immediately behind the step. Utilizing an upstream ramp can effectively control the flow in the presence of a crossflow jet. This upstream ramp mitigates the influence of the incoming mainstream flow, which tends to deflect the coolant jet upward, thereby facilitating adjustments to the coolant flow within the film cooling hole.

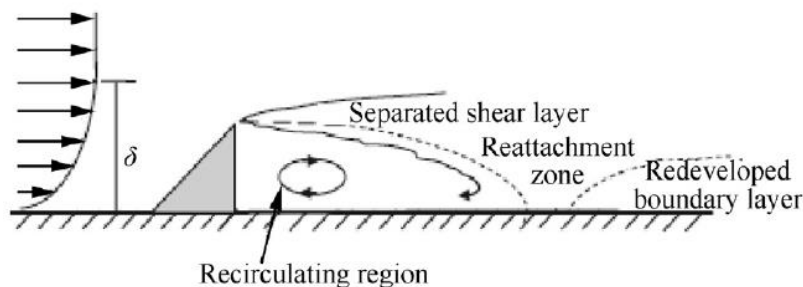


Figure 33 Schematic diagram of flow field over an upstream ramp [24]

Positioning the upstream ramp can reduce the pressure drop near the jet hole exit by mitigating the jetting effect within the cooling hole, as illustrated in Figure 33. As the upstream flow passes over the ramp, a region of low static pressure forms in front of the hole, as depicted in Figure 33(b). This low-pressure zone encourages the lateral spreading of the film cooling, increasing it by two or three times compared to cases without the ramp [106]. This demonstrates that modifying the approach of flow to the cooling hole can alter the interaction between the coolant and the mainstream flow. It provides inspiration for further advancements in this technique, aiming to strike a favourable balance between film cooling efficiency and aerodynamic loss.

Innovations in ramp designs for enhancing film cooling techniques extend beyond simple triangular or rectangular blocks placed upstream of film holes. Among these designs (Table 5), the Barchan-dune-shaped-ramp (BDSR) stands out due to its unique crescent shape when viewed from the top. Although several ramp designs have been explored for the same purpose of improving film cooling performance, this discussion will focus solely on the Barchan-dune-shaped-ramp (BDSR) design, as it is noted for its favourable aerodynamic profile in relation to upstream flow. Zhou and Hu [107] investigated the use of the BDSR design and qualitatively compared it to a baseline condition where no ramp was placed upstream of the hole, aiming to assess the enhancement achievable with the ramp.

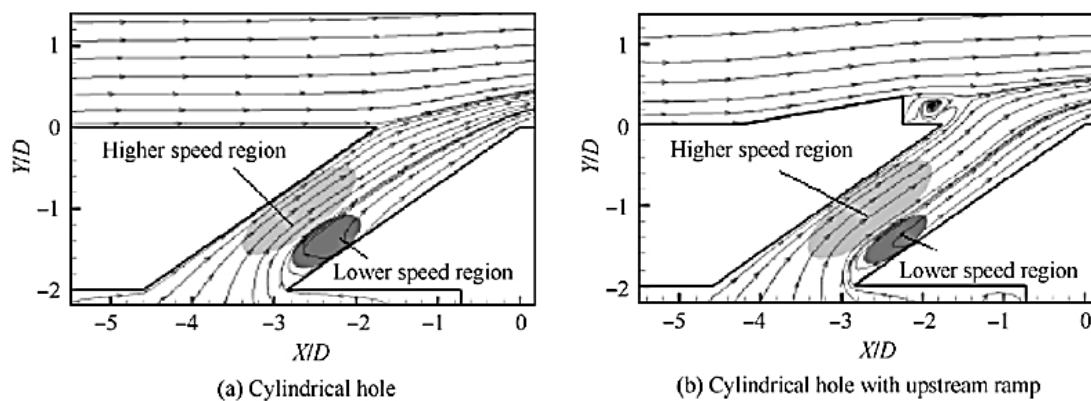


Figure 34 Streamlines and velocity vectors in an x-z plane that cross the cooling hole in the film. (Higher speed zone is indicated by lighter grey and lower speed regions with separation are indicated by darker grey) [106]

Table 5 Partial catalogue of the exploration other relating to the shaped ramps

Shape-ramp type	Reference Study
Curved ramp	Abdala & Elwekeel, [108]
Pyramid ramp	Hammami et al., [109]
Divided ramps	Zheng et al., [110]
Curved and wave-shape ramp	Zheng et al., [111]
Uneven-height ramp	Zhang et al., [112]
Sand-dune ramp	Zhou et al., [113]

The film cooling effectiveness contours obtained through pressure sensitive paint (PSP) measurements, as depicted in Figure 35, clearly illustrate the improvements brought about by the BDSR. At a low blowing ratio ($M=0.4$), the case without the ramp placement showed higher cooling effectiveness downstream of the hole compared to the case with the ramp, where higher cooling efficiency was mainly concentrated around the hole. However, the addition of the ramp facilitated lateral spreading of the film, extending beyond the hole's

diameter. This resulted in a broader film coverage, providing surface protection against the mainstream flow. The advantages of ramp placement became more pronounced as the blowing ratio increased ($M \geq 0.85$). In these cases, film cooling effectiveness and coverage remained superior to those without the ramp. The uniformity of film coverage was attributed to the formation of a low static pressure region, which encouraged lateral dispersion of the coolant exiting the hole and minimized the likelihood of coolant lift-off.

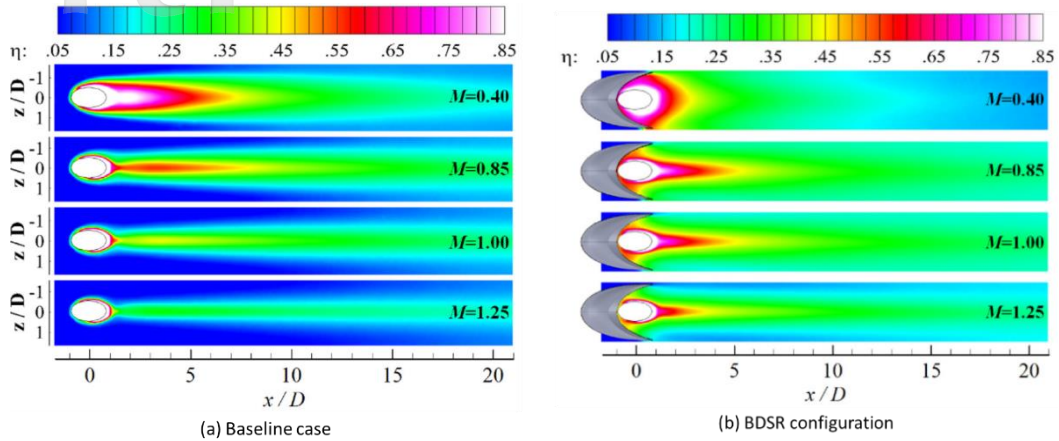


Figure 35 Cooling effectiveness distributions [107]

While the inclusion of a ramp has proven effective in mitigating the jetting effect and enhancing film cooling coverage, it's important to note that these improvements are primarily attributed to the interaction between the ramp and the mainstream flow, rather than the film hole itself [114,115]. Clearly, the angle and height of the ramp play a pivotal role in determining film cooling effectiveness [116]. If the ramp's angle or height is too excessive, it may result in the formation of a zone positioned too high, permitting mainstream flow to pass underneath it, which is an undesirable outcome. Conversely, if the angle or height is too modest, this zone may not fully develop, impeding the lateral spreading of the film, as illustrated in Figure 36(a).

The placement distance of the ramp from the coolant hole is also a critical factor that influences its performance [117]. If the ramp is situated too far from the hole, the zone forms in front of the hole, leading to the reattachment zone for the ramp forming on the hole itself. This situation can disrupt the coolant flow and promote further mixing between the mainstream flow and the coolant downstream. On the other hand, if the ramp is positioned too close to the hole, the zone that aids in film spreading may form directly over the coolant hole, potentially exacerbating the jetting effect and impeding film coverage, as depicted in Figure 36(b). Therefore, careful consideration of the design and placement of the ramp is essential, as it significantly impacts the interaction between the ramp and the mainstream flow.

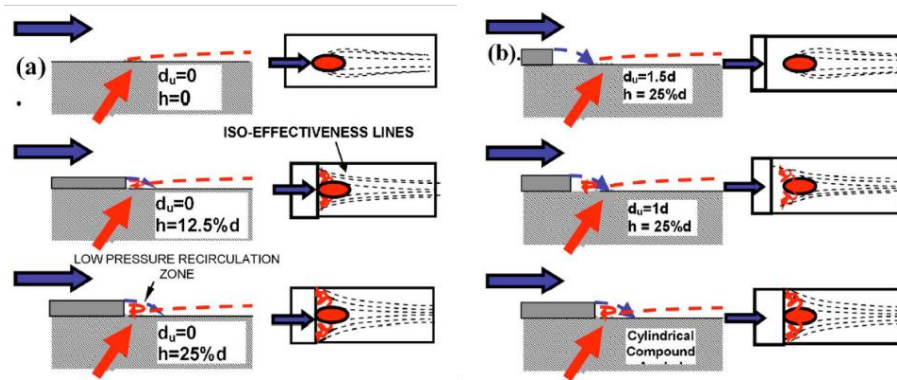


Figure 36 The efficiency of film cooling by trapping the coolant in a recirculation zone that is created right after the step. (a) effect of step height, h and (b) effect of distance of the upstream step from lead [117]

Trench or crater about a row of holes.

The placement of a coolant hole within a crater or trench has a significant impact on film cooling effectiveness and coverage area. Harrison and Bogard [118] have provided evidence that positioning the hole within a trench helps minimize the occurrence of coolant lift-off, particularly at high blowing ratios, as illustrated in

Figure 37. At low blowing ratios ($M=0.6$), there isn't a significant difference in flow separation from the surface between the trenched and untrenched hole configurations. In fact, the untrenched hole exhibits longer attachment

downstream of the hole compared to the trenched hole. This could be attributed to the higher jet momentum of the coolant in the untrenched hole, allowing it to attach further before detaching from the surface while interacting with the mainstream flow. However, at higher blowing ratios ($M \geq 1$), the lift-off event becomes clearly observable for the untrenched hole, whereas the trenched hole allows the coolant to remain attached to the surface. This is once again due to the reduction in jet momentum of the coolant exiting the trenched hole, which decreases to a level that permits the coolant to remain attached to the surface.

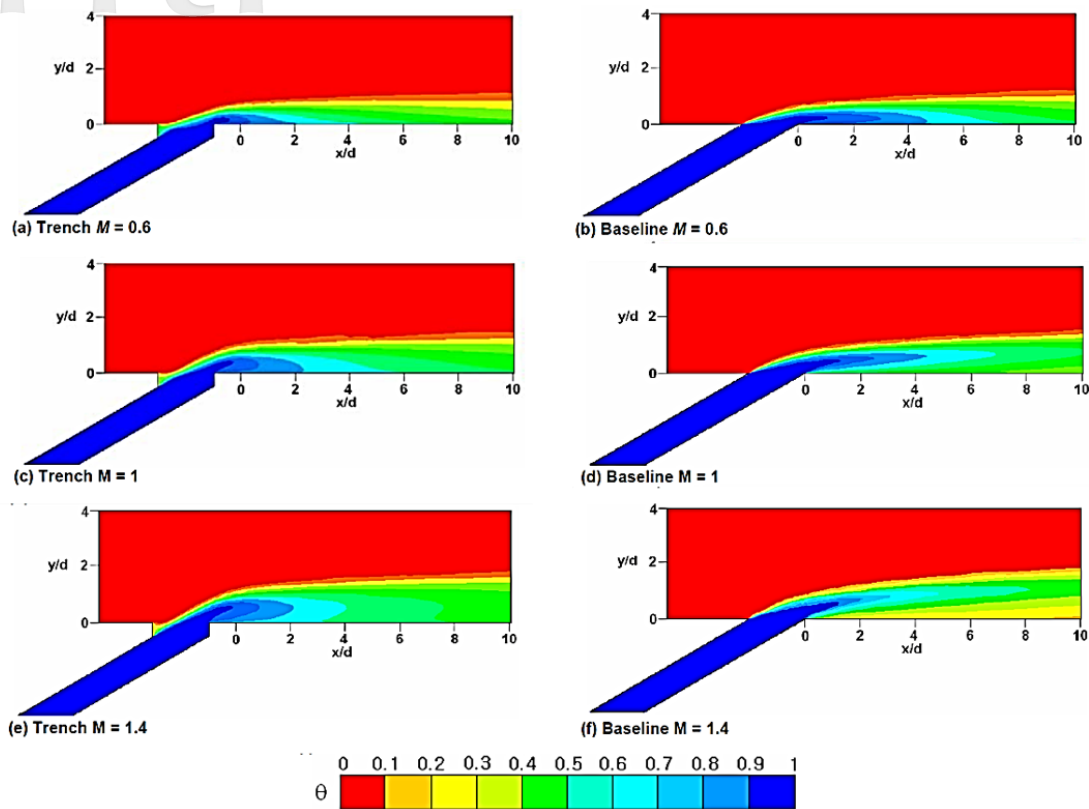


Figure 37 Trench and baseline holes centreline thermal profiles [118]

Just like the film holes and ramps discussed earlier, the design dimensions of the trench also play a crucial role in realizing its full potential. Lu et al., [119] took this factor into account and employed cylindrical holes to investigate the influence of trench width and depth (as detailed in Table 6 and Figure 38) on the effectiveness of film cooling. These findings were then compared with those of a fan-shaped hole without a trench.

Table 6 Summary of the width and depth of the trench studied by Lu et al., [119]

Baseline	Width	Depth
	Baseline un-trenched cylindrical hole	
Case '1'	$2D$	$0.5D$
Case '2'	$3D$	$0.5D$
Case '3'	$2D$	$0.75D$
Case '4'	$3D$	$0.75D$
Case '5'	$2D$	$1.0D$
Case '6'	$3D$	$1.0D$
Shaped hole	Un-trenched Fan shaped Hole	

In general, trenched holes tend to exhibit lower pressure drops, indicating that they minimize the jetting effect of the hole due to reduced jet momentum as the coolant exits the holes. Therefore, trenching the hole has been proven to enhance lateral dispersion of the film coolant and improve the average film cooling effectiveness compared to the baseline scenario where a

cylindrical hole was not trenched, as illustrated in Figure 39. The depth of the trench plays a critical role in reducing jet momentum, as the coolant contacts the trench's side before interacting with the mainstream flow.

Shallow trenches (Case 1) may appear advantageous at low blowing ratios compared to medium-depth trenches (Case 3). However, Case 3 offers superior lateral dispersion of coolant because, at low blowing ratios, it sufficiently reduces coolant jet momentum to enable better lateral extension. In contrast, Case 1 cannot fully reduce momentum, as the upper part of the coolant jet may not hit the trench's side and directly contacts the mainstream flow. However, this situation improves as the blowing ratio increases, with Case 1 displaying increased lateral dispersion like Case 3.

Deeper trenches (Case 5) may yield high efficiency and wide lateral coolant coverage at low blowing ratios but perform poorly as the blowing ratio increases, particularly far downstream from the hole. This could be attributed to the mainstream flow mixing with the coolant inside the trench. The mixing region within the coolant generally forms a swirling zone due to the creation of a low-static-pressure zone as the coolant contacts the trench's side. With increased trench depth, this zone is dragged downward, allowing the mainstream to enter the trench and mix with the coolant. As the blowing ratio further increases, this zone becomes more turbulent with increased mainstream flow interaction. Ultimately, the trapped coolant flows out of the trench with very low cooling effectiveness.

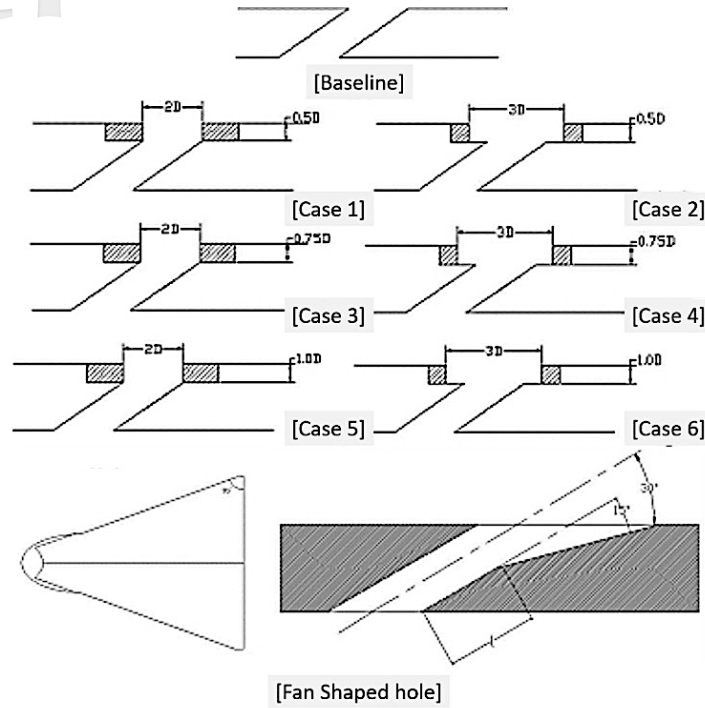


Figure 38 Different holes configurations studied by Lu et al., [119]

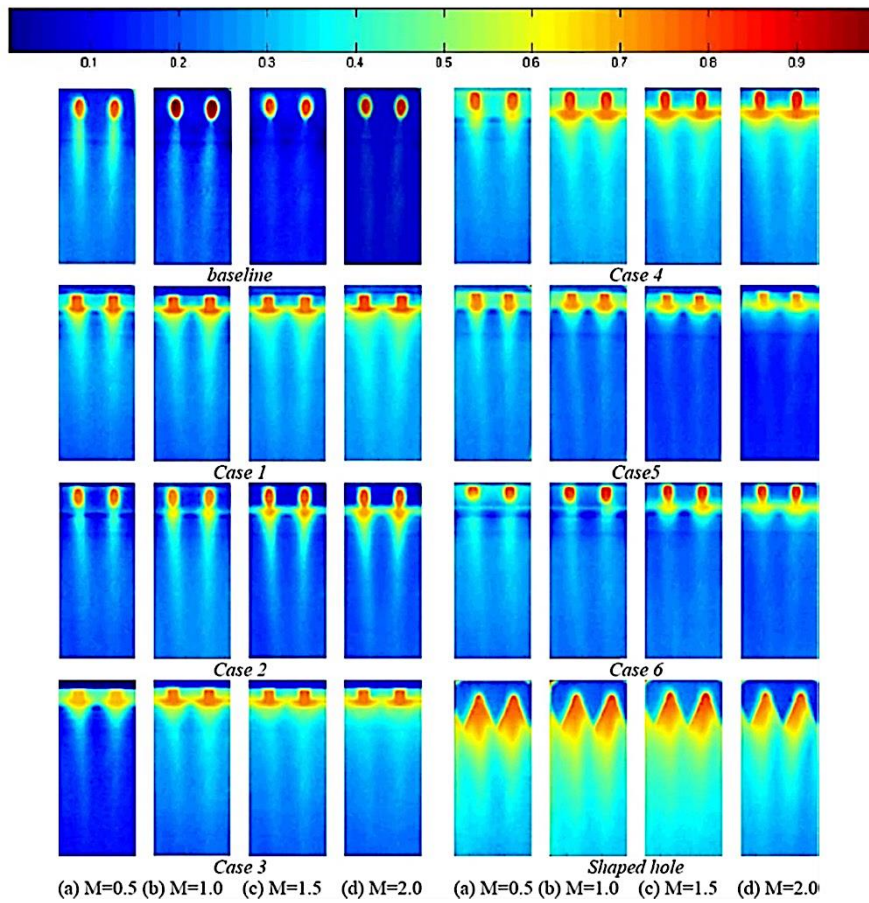


Figure 39 Film cooling effectiveness for each case at different blowing ratio [119]

The width of the trench also affects the formation of the low-static-pressure zone inside it. Narrow trenches (Case 3) do not exhibit as high lateral dispersion of coolant as wide trenches (Case 4). This may be due to the limited space in narrow trenches, preventing the low-static-pressure zone from fully developing and confining it within the narrow space. However, some wide trenches (Case 6) may promote lateral dispersion of coolant. Still, as the blowing ratio increases, coolant mixing inside wide trenches decreases compared to narrow trenches. This could result from the coolant exiting the trench without contacting its side, defeating the purpose of the trench.

Despite the promising results of trenching holes, there are limitations to what a simple cylindrical hole can achieve. Qualitative comparisons show that fan-shaped holes provide better cooling efficiency and larger film coverage than trenched holes, as shown in Figure 39. The wide exit of the fan-shaped hole helps keep the coolant attached to the surface by minimizing jet momentum. Additionally, the compound angle designed for the fan-shaped hole leads to more reliable lateral coverage, as discussed earlier.

Table 7 Configuration tested by Song et al., [120]

Configuration	Height of trench, H/d	Distance from hole exit to downstream sidewall, D/d	Radius of curvature of downstream sidewall, R/d
Baseline	-	-	-
Reference	0.8	0.75	0
1	0.4	0	0.2
2	0.4	1.5	0.2
3	1.2	0	0.2
4	1.2	1.5	0.2
5	0.8	0	0
6	0.8	1.5	0
7	0.8	0	0.4
8	0.8	1.5	0.4
9	0.4	0.75	0
10	1.2	0.75	0
11	0.4	0.75	0.4
12	1.2	0.75	0.4
13	0.8	0.75	0.2

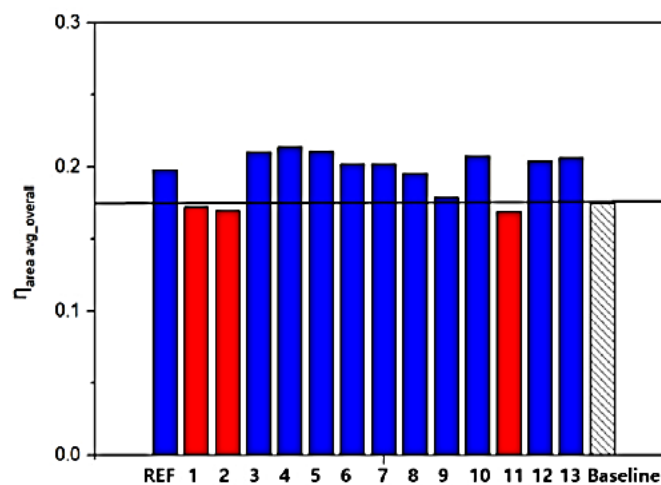


Figure 40 Comparison of averaged film cooling performance across the board at $M = 2.0$. [120]

Due to the limitations of what a simple cylindrical hole can achieve, Song et al., [120] considered trenching

the fan-shaped hole in various configurations, including variations in trench depth, distance from the hole exit to

the downstream sidewall, and radius of curvature of the downstream sidewall. They compared these trenched configurations with an un-trenched hole. The different trenching configurations are summarized in Table 7. Once again, trenching was found to enhance the cooling effectiveness of the hole, with most trench configurations elevating the average film cooling effectiveness compared to the baseline fan-shaped hole, except for configurations 1, 2, and 11 (Figure 40). In these cases, the height or depth of the trench was not sufficient to fully utilize the trench's potential.

Shallow trenches ($H/d \leq 0.5$) were unable to effectively reduce the jet momentum of the coolant exiting the hole, especially at higher blowing ratios. This is due because as for shallow trenches, some coolant that exiting the jet hole are not properly impinge on the trenches wall which was proposed to promote a recirculation inside the trench and directly penetrate the mainstream flow. This resulted in poor coolant recirculation inside the trench and inadequate lateral distribution of the coolant. The performance of other configurations was influenced by a combination of factors, including trench depth, distance from the hole exit to the downstream sidewall, and radius of curvature of the downstream sidewall.

For example, when quantitatively compared, configuration 6 exhibited higher film cooling effectiveness than configuration 8, even though both configurations had the same depth and width but different radii of curvature on the trench sidewall. The filleted edge of the trench sidewall in configuration 8 might not fully reduce the jet

momentum, as was achieved by the un-filleted trench in configuration 6. Some of the jet might not hit the sidewall and could directly penetrate the mainstream flow. However, this does not necessarily mean that the filleting process deteriorates the trench's film cooling performance. It suggests that the fillet may be more suitable for certain trench widths. This is supported by configuration 7, which had the same depth and radius of fillet as configuration 8 but with a narrower width. Configuration 7 exhibited the same or better film cooling effectiveness than configuration 6. This could be due to the fillet creating additional space for the formation of a recirculation zone, which might not occur without the fillet.

The design of the downstream sidewall edge of the trench has garnered attention from Oguntade et al., [121], who conducted a numerical comparison of various sidewall edge designs for the trench, as illustrated in Figure 41. The bevelled and rounded edge of the trench has been shown to effectively reduce the momentum of the coolant jet. This allows the coolant to maintain attachment to the wall surface and disperse uniformly in the lateral direction. This phenomenon is attributed to the Coanda effect, in which the flow has a natural tendency to remain attached to a wall, especially if the surface is convex or rounded. Additionally, it was anticipated that, for a given total coolant mass flow and surface area, higher surface-averaged cooling efficiency would be achieved by decreasing the coolant mass flow per hole and increasing the number of rows of holes.

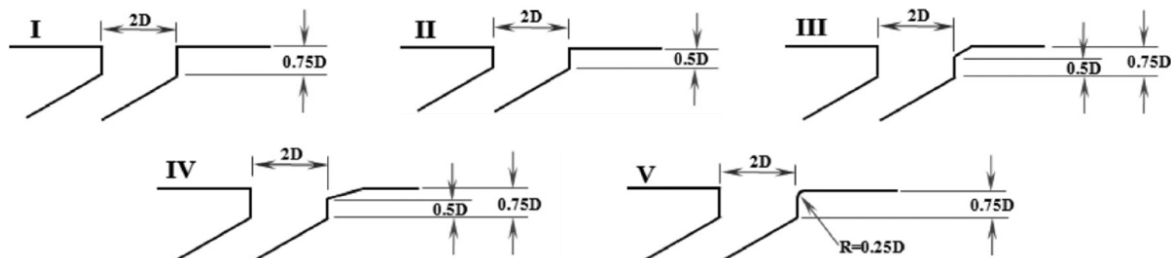


Figure 41 Trench outlet configuration [121]

IV. CONCLUSIONS

This paper presents a comprehensive review of the design and configuration of film cooling holes in gas turbine engines. The primary focus is on the critical issue of the interaction between the mainstream flow and the cooling jet, impacting various factors related to hole geometry, such as length-to-diameter ratio (L/D), exit to inlet cross-sectional area ratio (AR), pitch-to-diameter ratio (P/D), and the compound angle of the hole. Additionally, this paper examines modifications made upstream of the holes, such as vortex generators or the creation of trenches around rows of holes, to alter the aerodynamic interaction between mainstream flow and coolant.

Key findings include the observation that coolant jet detachment from the intended surface may occur at higher

flow velocities, potentially compromising the effectiveness of film cooling. The reduction of counter-rotating vortex pairs (CRVP), also known as kidney vortices, is identified as crucial for improving film cooling. Creating reverse-rotating kidney vortex pairs, referred to as anti-kidney vortex pairs, through well-designed cooling jet holes can help mitigate this issue, even at high blowing ratios.

Advancements in hole design over the years have evolved from simple cylindrical shapes to more complex configurations like Nekomimi, which demonstrated enhanced cooling performance. The effectiveness of film cooling varies for short holes ($L/D \leq 3$) due to underdeveloped coolant flow, while longer holes ($L/D > 3$) exhibit better performance thanks to fully developed coolant flow. Aspect ratio and pitch between holes influence coolant spreading, and compound angled holes improve lateral coverage.

As the blowing ratio ($M=1$) was maintained at a modest level, the contours of the measured adiabatic efficacy expanded as the area ratio increased. The effectiveness of the hole decreases as it approaches the trailing edge, which can be attributed to the phenomenon of mainstream ingestion and over-diffusion occurring in the diffusers of holes with increasing area ratios. This is mostly caused by the overpowering of coolant flow by the mainstream flow. Nonetheless, the increased breakout width of the larger AR hole diffusers resulted in a broader distribution of coolant along the end wall, particularly in the downstream region of the holes, so reducing the impact of mixing phenomena. In relation to hole pitch, it is observed that as jets converge downstream, a reduced spacing or pitch results in a greater coverage of surface area, irrespective of the diameter of the holes. The absence of flow interaction between adjacent holes results in the dependence of the covered area on the diameter of the holes when the pitch is very big. The alterations made to compound angles will impact the flow characteristics of the aperture. The compound angle orientation system involves the incorporation of a spanwise momentum component into the coolant. Consequently, the incorporation of compound angle holes yields a more homogeneous dispersion of film coverage along the spanwise axis. The presence of vortex forms in the downstream region of the jet significantly affects the distribution of adiabatic cooling efficacy and heat transfer coefficient on the cooling wall.

Innovations beyond standard hole shapes, such as Nekomimi, show promise in enhancing cooling performance. Upstream ramps reduce pressure drop at hole exits and promote lateral coolant spreading. Craters or trenches created near film cooling holes impact coolant distribution and effectiveness. However, there is no one-size-fits-all solution, and future research is expected to produce novel methods and optimizations for robust film cooling designs.

Based on literatures that haven't discussed in the current paper, it can be concluded that film cooling has evolved from many aspects of design parameters. However, the changes that were done throughout this evolution are not a silver bullet that can solve all of these technique flaws. The changes might improve in one way but lose on another; therefore, it was expected for future research to produce novel methods and optimizations that address the challenges and complexities of film cooling.

ACKNOWLEDGMENTS

The authors would like to thank the Ministry of Higher Education (MoHE) for the funding allocated in this project under the Malaysia Spain Innovation Programme (MySIP) No. 5540547.

REFERENCES

- [1] Sivapalan J, Mohd Rafie AS, Abu Talib AR, Gires E, Basri AA, Romli FI, Mohd Harithuddin AS, Sobri SA, Abdul Hamid MF, "The Aerodynamic Lift Performance Analysis of Channel-Wing Design for STOL Aircraft," *Journal of Aeronautics, Astronautics and Aviation*, Vol. 55, No. 3S, 2023, pp. 415-423.
- [2] Rafiul Alam JA, Abu Talib AR, Altarazi YSM, Yusaf T, Azami MH, Nik Mohd NAR, "Experimental Investigation on Gas Turbine Engine Performance using Alternative Fuel," *Journal of Aeronautics, Astronautics and Aviation*, Vol. 55, No. 3S, 2023, pp. 479-483.
- [3] Altarazi YSM, Abu Talib AR, Yu J, Gires E, Abdul Ghafir MF, Lucas J, Yusaf T, "Simulating Aero-engine Performance and Emissions Characteristics running on Green Diesel," *International Journal of Green Energy*, Vol. 20, No. 4, 2023, pp. 372-377.
- [4] Muhammad I, Abu Talib AR, "Experimental Investigation of Metal-Laminates with Aerogel in High-Temperature Application," *Journal of Aeronautics, Astronautics and Aviation*, Vol. 53, No. 2, 2021, pp. 121-128.
- [5] Muhammad I, Abu Talib AR, "Strength Behaviour of Silica Aerogel/Thermoset Polymer with Reinforced Fibre-metal Laminate Composites," *Journal of Aeronautics, Astronautics and Aviation*, Vol. 52, No. 1, 2020, pp. 15-24.
- [6] Rupesh P, Arulprakasajothi M, Raja K, Korem PR, Kaleshvali S, Dwivedi V, "Material selection for a gas turbine liner using MC 350-8 coating," *Materials Today*, Vol. 46, 2021, pp. 1235-1242.
- [7] Kim SH, Ahn KH, Park JS, Jung EY, Hwang KY, Cho HH, "Local heat and mass transfer measurements for multi-layered impingement/effusion cooling: Effects of pin spacing on the impingement and effusion plate," *International Journal of Heat and Mass Transfer*, Vol. 105, 2017, pp. 712-722.
- [8] Greifenstein M, Dreizler A, "Investigation of mixing processes of effusion cooling air and main flow in a single sector model gas turbine combustor at elevated pressure," *International Journal of Heat and Fluid Flow*, Vol. 88, 2021, pp. 108768.
- [9] Li L, Liu T, Peng XF, "Flow characteristics in an annular burner with fully film cooling," *Applied Thermal Engineering*, Vol. 25, No. 17-18, 2005, pp. 3013-3024.
- [10] Xu G, Liu Y, Luo X, Ma J, Li H, "Experimental investigation of transpiration cooling for sintered woven wire mesh structures," *International Journal of Heat and Mass Transfer*, Vol. 91, 2015, pp. 898-907.
- [11] Laraia M, Manna M, Cinque G, Martino PD, "A combustor liner cooling system design methodology based on a fluid/structure approach," *Applied Thermal Engineering*, Vol. 60, 2013, pp. 105-121.
- [12] Chi Z, Kan R, Ren J, Jiang H, "Experimental and numerical study of the anti-crossflows impingement cooling structure," *International Journal of Heat and Mass Transfer*, Vol. 64, 2013, pp. 567-580.
- [13] Nader S, "Paths to a low-carbon economy - The Masdar example," *Energy Procedia*, Vol. 1, No. 1,

- 2009, pp. 3951-3958.
- [14] Goldemberg J, "The promise of clean energy," *Energy Policy*, Vol. 34, No. 15, 2006, pp. 2185-2190.
- [15] Yıldız İ, "Fossil Fuels," *Comprehensive Energy Systems*, Elsevier, 2018, pp. 521-567.
- [16] Lee DS, Fahey DW, Forster PM, Newton PJ, Wit RCN, Lim LL, Owen B, Sausen R, "Aviation and global climate change in the 21st century," *Atmospheric Environment*, Vol. 43, No. 22-23, 2009, pp. 3520-3537.
- [17] Lee DS, Pitari G, Volker G, Gierens K, Penner J, Petzold A, Prather M, Schumann U, Bais AF, Berntsen T, Iachetti D, Lim LL, Sausen R, "Transport impacts on atmosphere and climate: Aviation," *Atmospheric Environment*, Vol. 44, No. 37, 2010, pp. 4678-4734.
- [18] Dessens O, Köhler MO, Rogers HL, Jones RL, Pyle JA, "Aviation and climate change," *Transport Policy: Air Transportation and the Environment*, Vol. 34, No. 1, 2014, pp. 14-20.
- [19] Khodayari S, Olsen C, Wuebbles DJ, "Evaluation of aviation NO_x induced radiative forcings for 2005 and 2050," *Atmospheric Environment*, Vol. 91, No. 1, 2014, pp. 95-103.
- [20] International Civil Aviation Organization, "Voluntary Emissions Trading for Aviation," 2007.
- [21] Liu Y, Sun X, Sethi V, Nalianda D, Li YG, Wang L, "Review of modern low emissions combustion technologies for aero gas turbine engines," *Progress in Aerospace Sciences*, Vol. 94, No. 1, 2017, pp. 12-45.
- [22] International Civil Aviation Organization, "Aviation Outlook: Local Air Quality Outlook," in ICAO Environment Report 2010, Montreal, Canada, 2010, pp. 27-30.
- [23] Wang Y, Wang W, Tao G, Li H, Zheng Y, Cui J, "Optimization of the semi-sphere vortex generator for film cooling using generative adversarial network," *International Journal of Heat and Mass Transfer*, Vol. 183, No. 4, 2022, pp.122026.
- [24] Zhang J, Zhang S, Wang C, Tan X, "Recent advances in film cooling enhancement: A review," *Chinese Journal of Aeronautics*, Vol. 33, No. 4, 2020, pp. 1119-1136.
- [25] Feist JP, A. Heyes L, Seeelt S, "Thermographic phosphor thermometry for film cooling studies in gas turbine combustors," Proceedings of the Institution of Mechanical Engineers, Part A: *Journal of Power and Energy*, Vol. 217, No. 2, 2003, pp. 193-200.
- [26] Arnold R, Suslov D, Haidn O, "Film Cooling of Accelerated Flow in a Subscale Combustion Chamber," *Journal of Propulsion and Power*, Vol. 25, No. 2, 2009, pp. 443-451.
- [27] Lihonga Q, Jingzhou Z, Xiaoming T, Minmina W, "Numerical investigation on adiabatic film cooling effectiveness and heat transfer coefficient for effusion cooling over a transverse corrugated surface," *Chinese Journal of Aeronautics*, Vol. 30, No. 2, 2017, pp. 277-284.
- [28] Tamunobere O, Acharya S, "Shroud Cooling with Blade Rotation Using Discrete Holes and an Upstream Slot," *Journal of Thermophysics and Heat Transfer*, Vol. 7, No. 4, 2016, pp. 1-8.
- [29] Collins M, Chana K, Povey T, "Application of Film Cooling to an Unshrouded High-Pressure Turbine Casing," *Journal of Turbomachinery*, Vol. 139, No. 6, 2017, pp. 061010.
- [30] Ho S, Goldstein RJ, Eckert ERG, "Film Cooling of a Gas Turbine Blade," *Journal of Engineering for Power*, Vol. 100, No. 7, 1978, pp. 476-481.
- [31] Bogard DG, Thole KA, "Gas Turbine Film Cooling," *Journal of Propulsion and Power*, Vol. 22, No. 2, 2006, pp. 249-270.
- [32] Town J, Straub DL, Black J, Shih TIP, "State-of-the-Art Cooling Technology for a Turbine Rotor Blade," *Journal of Turbomachinery*, Vol. 140, No. 7, 2018, pp. 0071007.
- [33] Stoll J, Straub J, "Film Cooling and Heat Transfer in Nozzles," *Journal of Turbomachinery*, Vol. 110, No. 1, 1988, pp. 57-65.
- [34] Lebedev VP, Lemanov VV, Terekhov VI, "Film-Cooling Efficiency in a Laval Nozzle Under Conditions of High Freestream Turbulence," *Journal of Heat Transfer*, Vol. 128, No. 6, 2006, pp. 571-579.
- [35] Yong S, Zhou ZJ, Xiong PC, "Numerical and experimental investigation of infrared radiation characteristics of a turbofan engine exhaust system with film cooling central body," *Aerospace Science and Technology*, Vol. 28, No. 1, 2013, pp. 281-288.
- [36] Chang H, Jing R, De JH, "Multi-parameter influence on combined-hole film cooling system," *International Journal of Heat and Mass Transfer*, Vol. 55, 2012, pp. 4232 - 4240.
- [37] Chen Z, Su X, Yuan X, "Trajectory and effectiveness of film cooling in end wall crossflow," *Aerospace Science and Technology*, Vol. 128, 2022, pp. 107795.
- [38] El-Gabry L, Heidmann J, Ameri A, "Penetration Characteristics of Film-Cooling Jets at High Blowing Ratio," *Journal of American Institute of Aeronautics and Astronautics*, Vol. 48, No. 5, 2010, pp. 1020-1024.
- [39] Zhang JZ, Zhu X, Huang DY, Wang CH, "Investigation on film cooling performance from a row of round-to-slot holes on flat plate," *International Journal of Thermal Sciences*, Vol. 118, 2017, pp. 207-225.
- [40] Graf L, Kleiser L, "Film Cooling Using Antikidney Vortex Pairs: Effect of Blowing Conditions and Yaw Angle on Cooling and Losses," *Journal of Turbomachinery*, Vol. 136, 2013, pp. 011008.
- [41] Wang C, Zhang J, Feng H, Huang Y, "Large eddy simulation of film cooling flow from a fan shaped hole," *Applied Thermal Engineering*, Vol. 129, 2018, pp. 855-870.
- [42] Haven BA, Yamagata DK, Kurosaka M, Yamawaki S, Maya T, "Anti-Kidney Pair of Vortices in Shaped Holes and Their Influence on Film Cooling Effectiveness," in ASME 1997

- International Gas Turbine and Aeroengine Congress and Exhibition, Orlando, Florida, USA, 1997.
- [43] Haven B, Kurosaka M, "Kidney and anti-kidney vortices in crossflow jets," *Journal of Fluid Mechanics*, Vol. 352, 1997, pp. 27-64.
- [44] Hyams DG, Leylek JH, "A Detailed Analysis of Film Cooling Physics: Part III - Streamwise Injection with Shaped Holes," *Journal of Turbomachinery*, Vol. 122, No. 1, 2000, pp. 122-132.
- [45] Bunker RS, "A Review of Shaped Hole Turbine Film-Cooling Technology," *Journal of Heat Transfer*, Vol. 127, No. 4, 2005, pp. 441-453.
- [46] Goldstein RJ, Eckert ERG, Burggraf F, "Effects of hole geometry and density on three-dimensional film cooling," *International Journal of Heat and Mass Transfer*, Vol. 17, No. 5, 1974, pp. 595-607.
- [47] Colban WF, Thole KA, Bogard D, "A film-cooling correlation for shaped holes on a flat-plate surface," *Journal of Turbomachinery*, Vol. 133, No. 1, 2011, pp. 011002.
- [48] Saumweber C, Schulz A, "Effect of Geometry Variations on the Cooling Performance of Fan-Shaped Cooling Holes," *Journal of Turbomachinery*, Vol. 134, No. 6, 2012, pp. 061008.
- [49] Wang C, Zhang J, Zhou J, Alting SA, "Prediction of film-cooling effectiveness based on support vector machine," *Applied Thermal Engineering*, Vol. 84, 2015, pp. 82-93.
- [50] Liu CL, Zhu HR, Bai JT, Xu DC, "Film Cooling Performance of Converging-Slot Holes with Different Exit-Entry Area Ratios," *Journal of Turbomachinery*, Vol. 133, No. 1, 2011, pp. 011020.
- [51] Yao Y, Zhang J, "Investigation on film cooling characteristics from a row of converging slot-holes on flat plate," *Science China Technological Sciences*, Vol. 54, No. 7, 2011, pp. 1793-1800.
- [52] Yao Y, Zhang JZ, Wang LP, "Film cooling on a gas turbine blade suction side with converging slot-hole," *International Journal of Thermal Sciences*, Vol. 65, 2013, pp. 267-279.
- [53] Yu Y, Zhou ZJ, Ming TX, "Numerical study of film cooling from converging slot-hole on a gas turbine blade suction side," *International Communications in Heat and Mass Transfer*, Vol. 52, 2014, pp. 61-72.
- [54] Pu J, Wang JH, Ma SY, Wu XY, "An experimental investigation of geometric effect of upstream converging slot-hole on end-wall film cooling and secondary vortex characteristics," *Experimental Thermal and Fluid Science*, Vol. 69, No. 2, 2015, pp. 58-72.
- [55] Wang C, Fan F, Zhang J, Huang Y, Feng H, "Large eddy simulation of film cooling flow from converging slot-holes," *International Journal of Thermal Sciences*, Vol. 126, No. 1, 2018, pp. 238-251.
- [56] Chang H, Jing R, De JH, "Multi-parameter influence on combined-hole film cooling system," *International Journal of Heat and Mass Transfer*, Vol. 55, No. 15, 2012, pp. 4232-4240.
- [57] Kim SM, Lee KD, Kim KY, "A comparative analysis of various shaped film-cooling holes," *Journal of Heat and Mass Transfer*, Vol. 48, No. 11, 2012, pp. 1929-1939.
- [58] Lee KD, Kim KY, "Performance Evaluation of a Novel Film-Cooling Hole," *Journal of Heat Transfer*, Vol. 134, No. 10, 2012, pp. 101702.
- [59] Kusterer K, Tekin N, Bohn D, Sugimoto T, Tanaka R, Kazari M, "Experimental and Numerical Investigations of the Nekomimi Film Cooling Technology," in ASME Turbo Expo 2012: Turbine Technical Conference and Exposition, Copenhagen, Denmark, 2012.
- [60] Kusterer K, Tekin N, Reiners F, Bohn D, Sugimoto T, Tanaka R, Kazari M, "Highest-Efficient Film Cooling by Improved NEKOMIMI Film Cooling Holes: Part 1 — Ambient Air Flow Conditions," in ASME Turbo Expo 2013: Turbine Technical Conference and Exposition, San Antonio, Texas, USA, 2013.
- [61] Kusterer K, Tekin N, Kasiri A, Bohn D, Sugimoto T, Tanaka R, Kazari M, "Highest-Efficient Film Cooling by Improved NEKOMIMI Film Cooling Holes: Part 2 - Hot Gas Flow Conditions," in ASME Turbo Expo 2013: Turbine Technical Conference and Exposition, San Antonio, Texas, USA, 2013.
- [62] Davidson FT, Macher DAK, Bogard DG, "Film Cooling with a Thermal Barrier Coating: Round Holes, Craters, and Trenches," *Journal of Turbomachinery*, Vol. 136, No. 4, 2014, pp. 0410074.
- [63] Kalghatgi P, Acharya S, "Improved film cooling effectiveness Acharya with a round film cooling hole embedded in a contoured crater," *Journal of Turbomachinery*, Vol. 137, No. 10, 2015, pp. 101006.
- [64] Kalghatgi P, Acharya S, "Flow Dynamics of a Film Cooling Jet Issued from a Round Hole Embedded in Contoured Crater," *Journal of Turbomachinery*, Vol. 141, No. 8, 2019, pp. 081006.
- [65] Kim JH, Kim KY, "Surrogate-based optimization of a cratered cylindrical hole to enhance film-cooling effectiveness," *Journal of Thermal Science and Technology*, Vol. 11, No. 2, 2016, pp. JTST0025.
- [66] An BT, Liu JJ, Zhang XD, Zhou SJ, Zhang C, "Film cooling effectiveness measurements of a near surface streamwise diffusion hole," *International Journal of Heat and Mass Transfer*, Vol. 103, 2016, pp. 1-13.
- [67] Feng HK, Wang CH, Fan FS, Zhang JZ, "Optimization Research of Film Cooling Structures with Cratered Cylindrical Hole," *Tuijin Jishu/ Journal of Propulsion Technology*, Vol. 40, No. 5, 2019, pp. 1099-1106.

- [68] Yang X, Liu Z, Feng Z, "Numerical evaluation of novel shaped holes for enhancing film cooling performance," *Journal of Heat Transfer*, Vol. 137, No. 7, 2015, pp. 071701.
- [69] Khajehhasani S, Jubran BA, "Numerical Assessment of the Film Cooling Through Novel Sister-Shaped Single-Hole Schemes," *Numerical Heat Transfer*, Vol. 67, No. 4, 2015, pp. 414-435.
- [70] Ramesh S, Ramirez DG, Ekkad SV, Alvin MA, "Analysis of film cooling performance of advanced tripod hole geometries with and without manufacturing features," *International Journal of Heat and Mass Transfer*, Vol. 94, No. 4, 2016, pp. 9-19.
- [71] Chi Z, Ren J, Jiang H, Zang S, "Geometrical Optimization and Experimental Validation of a Tripod Film Cooling Hole with Asymmetric Side Holes," *Journal of Heat Transfer*, Vol. 138, No. 6, 2016, pp. 061701.
- [72] Ramesh S, LeBlanc C, Narzary D, Ekkad S, Alvin MA, "Film Cooling Performance of Tripod Antivortex Injection Holes Over the Pressure and Suction Surfaces of a Nozzle Guide Vane," *Journal of Thermal Science and Engineering Applications*, Vol. 9, No. 2, 2016, pp. 011006.
- [73] Zhang JZ, Zhu XD, Huang Y, Wang CH, "Investigation on film cooling performance from a row of round-to-slot holes on flat plate," *International Journal of Thermal Sciences*, Vol. 118, 2017, pp. 207-225.
- [74] Huang Y, Zhang J, Wang CH, "Shape-optimization of round-to-slot holes for improving film cooling effectiveness on a flat surface," *Heat and Mass Transfer*, Vol. 54, No. 6, 2018, pp. 1741-1754.
- [75] Zhu XD, Zhang JZ, Tan XM, "Numerical assessment of round-to-slot film cooling performances on a turbine blade under engine representative conditions," *International Communications in Heat and Mass Transfer*, Vol. 100, 2019, pp. 98-110.
- [76] Zhu R, Simon TW, Xie G, "Influence of secondary hole injection angle on enhancement of film cooling effectiveness with horn-shaped or cylindrical primary holes," *Numerical Heat Transfer, Part A: Applications*, Vol. 74, No. 5, 2018, pp. 1207-1227.
- [77] Saumweber C, Schulz A, "Effect of geometry variations on the cooling performance of fan-shaped cooling holes," *Journal of Turbomachinery*, Vol. 134, No. 6, 2012, pp. 061008.
- [78] Gritsch M, Colban W, Schär H, Döbbling K, "Effect of Hole Geometry on the Thermal Performance of Fan-Shaped Film Cooling Holes," *Journal of Turbomachinery*, Vol. 127, No. 4, 2005, pp. 718-725.
- [79] Singh K, Premachandran B, Ravi MR, "Experimental assessment of film cooling performance of short cylindrical holes on a flat surface," *Heat and Mass Transfer*, Vol. 52, No. 11 2016, pp. 2849-2862.
- [80] Li W, Shi W, Li X, Ren J, Jiang H, "On the Flow Structures and Adiabatic Film Effectiveness for Simple and Compound Angle Hole with Varied Length-to- Hole with Varied Length-to- Simulation and Pressure- Sensitive Paint Techniques," *Journal of Heat Transfer*, Vol. 139, No. 12, 2017, pp. 122201.
- [81] Li W, Lu X, Li X, Ren J, Jiang H, "High resolution measurements of film cooling performance of simple and compound angle cylindrical holes with varying hole length-to-diameter ratio - Part I: Adiabatic film effectiveness," *International Journal of Thermal Sciences*, Vol. 124, 2018, pp. 146-161.
- [82] Li W, Li X, Ren J, Jiang H, "Length to diameter ratio effect on heat transfer performance of simple and compound angle holes in thin-wall airfoil cooling," *International Journal of Heat and Mass Transfer*, Vol. 127, 2018, pp. 867-879.
- [83] Haydt S, Lynch S, Lewis S, "The Effect of Area Ratio Change Via Increased Hole Length for Shaped Film Cooling Holes with Constant Expansion Angles," *Journal of Turbomachinery*, Vol. 140, No. 5, 2017, pp. 051002.
- [84] Kim JH, Kim KY, "Film-cooling performance of converged-inlet hole shapes," *International Journal of Thermal Sciences*, Vol. 124, 2018, pp. 196-211.
- [85] Bogard D, Schmidt DL, Tabbita M, "Characterization and Laboratory Simulation of Turbine Airfoil Surface Roughness and Associated Heat Transfer," *Journal of Turbomachinery*, Vol. 120, No. 2, 1998, pp. 337-342.
- [86] Chen X, Wang Y, Long Y, Weng S, "Effect of partial blockage on flow and heat transfer of film cooling with cylindrical and fan-shaped holes," *International Journal of Thermal Sciences*, Vol. 164, 2021, pp. 106866.
- [87] Rouina S, Ravelli S, Barigozzi G, "An Experimental Study of Flat Plate Film Cooling with Cylindrical Holes by Using PIV, HWA and PSP Techniques," in Second International Conference on Material Science, Smart Structures and Applications: ICMSS-2019, Modena, Italy, 2019.
- [88] Liu CL, Zhu HR, Zhang ZW, Xu DC, "Experimental investigation on the leading-edge film cooling of cylindrical and laid-back holes with different hole pitches," *International Journal of Heat and Mass Transfer*, Vol. 55, No. 23-24, 2012, pp. 6832-6845.
- [89] Zuniga H. A., and Kapat J. S., "Effect of Increasing Pitch-to-Diameter Ratio on the Film Cooling Effectiveness of Shaped and Cylindrical Holes Embedded in Trenches," in ASME Turbo Expo 2009: Power for Land, Sea, and Air, Orlando, Florida, USA, 2009.
- [90] Ahn J, Jung IS, Lee JS, "Film cooling from two rows of holes with opposite orientation angles: injectant behavior and adiabatic film cooling effectiveness," *International Journal of Heat and Fluid Flow*, Vol. 24, No. 1, 2003, pp. 91-99.

- [91] Abdelmohimen MAH, "Improving film cooling from compound angle holes by adding secondary holes branched out from the main holes," *Heat and Mass Transfer*, Vol. 12, No. 5, 2017, pp. 1-11.
- [92] Lee SW, Kim YB, Lee JS, "Flow Characteristics and Aerodynamic Losses of Film-Cooling Jets with Compound Angle Orientations," *Journal of Turbomachinery*, Vol. 119, No. 2, 1997, pp. 310-319.
- [93] Aga V, Abhari RS, "Influence of Flow Structure on Compound Angled Film Cooling Effectiveness and Heat Transfer," *Journal of Turbomachinery*, Vol. 133, No. 3, 2011, pp. 031029.
- [94] Kusterer K, Bohn D, Sugimoto T, Tanaka R, "Double-Jet Ejection of Cooling Air for Improved Film Cooling," *Journal of Turbomachinery*, Vol. 129, No. 4, 2007, pp. 809-815.
- [95] Kusterer K, Elyas A, Bohn D, Sugimoto T, Tanaka R, "Double-Jet Film-Cooling for Highly Efficient Film-Cooling with Low Blowing Ratios," in ASME Turbo Expo 2008: Power for Land, Sea, and Air, Berlin, Germany, 2008.
- [96] Kusterer K., Elyas A., Bohn D., Sugimoto T., Tanaka R, Kazari M, "A Parametric Study on the Influence of the Lateral Ejection Angle of Double-Jet Holes on the Film Cooling Effectiveness for High Blowing Ratios," in ASME Turbo Expo 2009: Power for Land, Sea, and Air, Orlando, Florida, USA, 2009.
- [97] Yao J, Xu J, Zhang K, Lei J, Wright L, "Effect of Density Ratio on Film-Cooling Effectiveness Distribution and Its Uniformity for Several Hole Geometries on A Flat Plate," *Journal of Turbomachinery*, Vol. 145, No. 5, 2018, pp. 051008.
- [98] Cho MY, Seo HS, Kim YJ, "Effect of Hole Pitch Ratio and Compound Angle on the Thermal Flow Fields of Double-Jet Film Cooling Hole," in ASME 2014 4th Joint US-European Fluids Engineering Division Summer Meeting collocated with the ASME 2014 12th International Conference on Nanochannels, Microchannels, and Minichannels, Chicago, Illinois, USA, 2014.
- [99] Yao J, Su P, He J, Wu J, Lei J, Fang Y, "Experimental and numerical investigations on double-jet film-cooling with different mainstream incidence angles," *Applied Thermal Engineering*, Vol. 166, 2020, pp. 114737.
- [100] He J, Yang JYX, Duan J, Lei J, Xie G, "Effects of mainstream attack angles on film-cooling effectiveness of double-jet film-cooling," *International Journal of Thermal Sciences*, Vol. 149, 2020, pp. 106183.
- [101] Wang Z, Liu J., An BT, Chao Z, "Effects of Axial Row-Spacing for Double-Jet Film-Cooling on the Cooling Effectiveness," in ASME 2011 Turbo Expo: Turbine Technical Conference and Exposition, Vancouver, British Columbia, Canada, 2011.
- [102] Yao J, Zhang K, Wu J, Lei J, Fang Y, Wright L, "An experimental investigation on streamwise distance and density ratio effects on double-jet film-cooling," *Applied Thermal Engineering*, Vol. 156, No. 2, 2019, pp. 410-421.
- [103] Yao J, Xu J, Zhang K, Lei J, Wright LM, "Interaction of Flow and Film-Cooling Effectiveness Between Double-Jet Film-Cooling Holes with Various Spanwise Distances," *Journal of Turbomachinery*, Vol. 140, No. 12, 2018, pp. 121011.
- [104] He J, Yao J, Yang X, Zhang K, Lei J, Xie G, "Investigation on overall performance of double-jet film cooling holes with various spanwise distance," *International Journal of Thermal Sciences*, Vol. 183, 2023, pp. 107841.
- [105] Kusterer K, Elyas A, Bohn D, Sugimoto T, Tanaka R, Kazari M, "The NEKOMIMI cooling technology: Cooling holes with ears for high-efficient film cooling," in ASME 2011 Turbo Expo: Turbine Technical Conference and Exposition, Vancouver, British Columbia, Canada, 2011.
- [106] Na S, Shih TIP, "Increasing adiabatic film-cooling effectiveness by using an upstream ramp," *Journal of Heat Transfer*, Vol. 129, No. 4, 2007, pp. 464-471.
- [107] Zhou W, Hu H, "Improvements of film cooling effectiveness by using Barchan dune shaped ramps," *International Journal of Heat and Mass Transfer*, Vol. 103, 2016, pp. 443-456.
- [108] Abdalaa MM, Elwekeel FNM, "An influence of novel upstream steps on film cooling performance," *International Journal of Heat and Mass Transfer*, Vol. 93, 2016, pp. 86-96.
- [109] Hammami Z, Dellil ZA, Nemdili F, Azzi A, "Improving adiabatic film-cooling effectiveness by using an upstream pyramid," *Computational Thermal Sciences*, Vol. 8, No. 2, 2016, pp. 135-146.
- [110] Zheng D, Wang X, Yuan FZQ, "Numerical investigation on the effects of the divided steps on film cooling performance," *Applied Thermal Engineering*, Vol. 124, 2017, pp. 652-662.
- [111] Zheng D, Wang X, Zhang F, Zhou J, Yuan Q, "The Effect of Upstream Ramps with Different Shapes on Film Cooling Efficiency," in ASME Turbo Expo 2017: Turbomachinery Technical Conference and Exposition, Charlotte, North Carolina, USA, 2017.
- [112] Zhang F, Wang X, Li J, "The effects of upstream steps with unevenly spanwise distributed height on rectangular hole film cooling performance," *International Journal of Heat and Mass Transfer*, Vol. 102, 2016, pp. 1209-1221.
- [113] Zhou W, Peng D, Wen X, Liu Y, Hu H, "Unsteady analysis of adiabatic film cooling effectiveness behind circular, shaped, and sand-dune-inspired film cooling holes: Measurement using fast-response pressure-sensitive paint," *International Journal of Heat and Mass Transfer*, Vol. 125, 2018, pp. 1003-1016.
- [114] Barigozzi G, Franchini G, Perdichizzi A, "The Effect of an Upstream Ramp on Cylindrical and Fan-Shaped Hole Film Cooling: Part I -

Aerodynamic Results,” in ASME Turbo Expo 2007: Power for Land, Sea, and Air, Montreal, Canada, 2009.

- [115] Barigozzi G, Franchini G, and Perdichizzi A, “The Effect of an Upstream Ramp on Cylindrical and Fan-Shaped Hole Film Cooling: Part II - Adiabatic Effectiveness Results,” in ASME Turbo Expo 2007: Power for Land, Sea, and Air, Montreal, Canada, 2007.
- [116] Chen SP, Hyu MK, Shih TIP, “Effects of upstream ramp on the performance of film cooling,” *International Journal of Thermal Sciences*, Vol. 50, No. 6, 2011, pp. 1085-1094.
- [117] Rallabandi P, Grizzle J, Han JC, “Effect of upstream step on flat plate film-cooling effectiveness using PSP,” *Journal of Turbomachinery*, Vol. 133, No. 4, 2011, pp. 041024.
- [118] Harrison KL, Bogard D, “CFD Predictions of Film Cooling Adiabatic Effectiveness for Cylindrical Holes Embedded in Narrow and Wide Transverse Trenches,” in ASME Turbo Expo 2007: Power for Land, Sea, and Air, Montreal, Canada, 2007.
- [119] Lu Y, Dhungel A, Ekkad SV, Bunker RS, “Effect of Trench Width and Depth on Film Cooling from Cylindrical Holes Embedded in Trenches,” *Journal of Turbomachinery*, Vol. 131, No. 1, 2009, pp. 011003.
- [120] Song YJ, Park SH, Kang YJ, Kwak JS, “Effects of trench configuration on the film cooling effectiveness of a fan-shaped hole,” *International Journal of Heat and Mass Transfer*, Vol. 178, 2021, pp. 121655.
- [121] Oguntade HI, Andrews GE, Burns AD, Ingham DB, Pourkashanian M, “Improved Trench Film Cooling with Shaped Trench Outlets,” *Journal of Turbomachinery*, Vol. 135, No. 2, 2013, pp. 021009.